

The Effect of Relative Flow on the Asymmetric Structure in the Interior of Hurricanes

MORRIS A. BENDER

Geophysical Fluid Dynamics Laboratory/NOAA, Princeton University, Princeton, New Jersey

(Manuscript received 2 February 1996, in final form 2 October 1996)

ABSTRACT

Asymmetric structure of tropical cyclones simulated by the Geophysical Fluid Dynamics Laboratory high-resolution triply nested movable-mesh hurricane model was analyzed. Emphasis was placed on the quasi-steady component of the asymmetric structure in the region of the eyewall. It was found that the asymmetry was primarily caused by the relative wind, that is, the flow entering and leaving the storm region relative to the moving storm. A set of idealized numerical experiments was first performed both with a constant and a variable Coriolis parameter (f) and the addition of basic flows that were either constant or sheared with height. Analysis was then made for one case of Hurricane Gilbert (1988) to demonstrate that the quasi-steady asymmetric structure analyzed in the idealized studies could be identified in this real data case.

Vorticity analysis in the variable f experiment indicated that quasi-steady asymmetries resulted in the eyewall region through the effect of vorticity advection due to differences between the beta gyre flow in the lower free atmosphere and the storm motion. This was roughly matched with a persistent area of divergence and vorticity compression in the lower free atmosphere ahead of the storm and enhanced convergence and vorticity stretching to the rear. An asymmetric structure in the upward motion and accumulated precipitation, when averaged over a sufficiently long period of time, exhibited a corresponding maximum in the eyewall's rear quadrant.

With the addition of an easterly basic flow, a pronounced change in the asymmetry of the time-averaged boundary layer convergence resulted, with maximum convergence located ahead of the storm. However, the asymmetries in the average vertical motion in the middle troposphere and accumulated precipitation were more affected by the convergence field in the lower free atmosphere produced by the relative flow there. The relative flow depended on both the basic and beta gyre flow. With the addition of an easterly vertical shear to the easterly basic flow, the storm moved faster than the lower-level winds, and strong relative wind was from the front to the rear in the lower free atmosphere and from the opposite direction in the outflow layer aloft. As a result, the upward motion was significantly increased in the front of the storm and reduced in the rear, and the precipitation maximum shifted to the left front quadrant.

Overall, analysis results suggest that the flow relative to the storm motion is an important factor contributing to the formation of quasi-steady asymmetries in the convergence and vertical motion fields, as well as in the mean precipitation pattern of tropical cyclones.

1. Introduction

The subject of asymmetry in the structure of tropical cyclones has received increased attention in recent years in the literature both through observational (e.g., Burpee and Black 1989; Marks et al. 1992; Franklin et al. 1993) and theoretical studies (e.g., Chan and Williams 1987; Fiorino and Elsberry 1989; Smith and Ulrich 1990; Peng and Williams 1990).

Many observational studies have demonstrated that the circulation and the convection in the interior core region of tropical cyclones (i.e., the eye, eyewall, and immediate surrounding area) often have a highly asymmetric structure. Frank (1984) noted marked asymmetries in the kinematic fields of Hurricane Frederic with a strong concentration of inflow northeast of the center

and maximum outflow toward the southwest quadrant at all radii. Investigation of the three-dimensional wind field in the inner core of Hurricane Norbert (Marks et al. 1992) and Hurricane Gloria (Franklin et al. 1993) revealed a highly asymmetric wind distribution that varied significantly with altitude. In early observational studies of the asymmetric precipitation distributions of tropical cyclones (e.g., Cline 1926; Miller 1958), hourly rain gauge data were composited for landfalling storms. Although the rainfall rates were found to be largest ahead and to the right of the storm center, Cline found the rainfall maximum for stationary storms tended to shift toward the rear of the center. Frank (1977) composited rainfall data from 13 small islands in the western North Pacific where the effect of land on the tropical cyclone was minimal. No large asymmetries were noted in Frank's study, although the rainfall was slightly higher in the right rear quadrant. In more recent studies, reflectivity data from airborne radar systems revealed large asymmetries in the rainfall rate for Hurricane Allen

Corresponding author address: Dr. Morris A. Bender, GFDL/NOAA, Princeton University, P.O. Box 308, Princeton, NJ 08542.
E-mail: mb@gfdl.gov

(Marks 1985), Hurricanes Alicia and Elena (Burpee and Black 1989), and Hurricane Norbert (Houze et al. 1992). In Hurricanes Elena and Allen, the location of the maximum rainfall remained in the right front quadrant while shifting from the left side to the right front quadrant in Hurricane Alicia. In Hurricane Norbert (Houze et al. 1992), the maximum radar reflectivity tended to be located either to the rear of the storm or to the left of the storm center. These studies indeed confirm that a large variability exists in the precipitation distribution between storms, since many factors influence their asymmetric distribution.

Through the integration of barotropic models (e.g., Chan and Williams 1987; Smith et al. 1990), it has been shown that an initially symmetric barotropic vortex on a beta plane will develop an asymmetric structure (commonly referred to as a beta gyre). Although the gyres are located in the outer area of the storm, the asymmetric flow associated with them causes vortex propagation at about $2\text{--}4\text{ m s}^{-1}$ in basically a northwestward direction (i.e., the beta effect). In integrations with barotropic models, the beta-gyre structure tends to be nearly steady after a day or two since the gyre produces an effect that counterbalances an effect of constant forcing, that is, the advection of planetary vorticity by the vortex's symmetric circulation. Beta gyres have also been observed in three-dimensional baroclinic models (Wang and Li 1992), and their possible role in storm movement in a baroclinic model has been discussed by Bender et al. (1993). In addition, Holland (1984) indicated close agreement between the motion of observed storms and a combination of vortex advection by the basic current and the beta effect. These results suggest that the beta-gyre structure identified in barotropic models is also present in baroclinic vortices, despite the presence of strong transient asymmetric features such as rotating convective cells.

Roughly speaking, a baroclinic vortex moves by the deep layer mean wind near the center. At a certain level of the atmosphere, there may exist a significant difference between the vortex motion and the flow at that particular level. The resulting flow that moves through the storm region at that vertical level relative to the moving storm (the relative wind) may result in steady vorticity forcing in the interior of the tropical cyclone. Therefore, the relative wind can generate quasi-steady asymmetries as well. Investigation of this mechanism will be the primary focus of this study. In real data studies the asymmetric relative wind was analyzed in various vertical levels for Hurricane Norbert (Marks et al. 1992) and Hurricane Gloria (Franklin et al. 1993). Their results suggested that the orientation of the shear vector of the asymmetric flow was the primary mechanism in the generation of asymmetries in the eyewall convection of hurricanes. In Hurricane Norbert the relative environmental flow in the direction of the storm motion was most important, while in Hurricane Gloria the cross-track component dominated (e.g., southwest-

erly shear) as the hurricane moved northwest. A similar type of relationship was proposed by Willoughby et al. (1984) in their study of spiral band structure in Hurricane Gert (1981). In their analysis, a pattern of convergence and divergence was produced on the east and west sides of the eyewall by the movement of the environmental flow through the vortex core at the lower levels. Using a simple slab boundary layer model of constant depth, Shapiro (1983) found that the storm motion produced enhanced convergence in the boundary layer in the front of translating storms. However, the theoretical study of Shapiro (1983) did not include the effects of vertical wind shear.

In the present numerical study, profiles of relative winds that rely on the environmental flow and their relation to asymmetries will be examined. Since the beta-gyre flow in baroclinic models will change with height in conjunction with the storm's tangential wind, the beta gyre may lead to an important contribution to the asymmetries in the interior region of tropical cyclones. This relationship will be analyzed in detail. Finally, it is noted here that the present investigation is focused on the mechanisms that contribute to the asymmetric structure rather than on mechanisms of vortex motion.

A brief description of the tropical cyclone model, experimental design, and experimental strategy will be outlined in section 2. A discussion of the relative wind and some of the terms used in this study will be presented in section 3. In section 4 the experimental results will be shown, first presenting the asymmetries in the interior of the tropical cyclones introduced by the beta gyre alone. Next, the asymmetries involving effects of basic flows will be presented, followed by discussion made of the asymmetric structure in one real data case of Hurricane Gilbert (1988). Throughout the present study, the asymmetries in the divergence field and the precipitation distribution will be emphasized. A brief summary with some concluding remarks will be the subject of section 5.

2. Model description, initial conditions, and experimental design

a. Model description and initial conditions

The triply nested, movable-mesh model described by Kurihara and Bender (1980) was used for this study. Specific model details have been outlined in previous publications (e.g., Tuleya et al. 1984; Bender et al. 1987) and are identical to the version of the atmospheric model used in Bender et al. (1993a, hereafter referred to as BGK). The model is a primitive equation model formulated in latitude, longitude, and σ coordinates, with 18 levels in the vertical. A summary of the sigma levels is given in Table 1 of Kurihara et al. (1990). The integration domain is also identical to BGK with the grid system for each of the three meshes summarized in Table

TABLE 1. Grid system of the triply nested mesh hurricane model.

Mesh	Grid resolution (degrees)	Domain size				Time step (s)
		Longitude (degrees)	Longitude (points)	Latitude (degrees)	Latitude (points)	
1	1	55	(55)	55	(55)	120
2	1/3	15	(45)	15	(45)	40
3	1/6	8½	(50)	8½	(50)	20

1. The model physics include cumulus parameterization described by Kurihara (1973) with some additional modifications (Kurihara and Bender 1980, appendix C), a Monin–Obukhov scheme for the surface flux calculation, and the Mellor and Yamada (1974) level-2 turbulence closure scheme for the vertical diffusion, with a background diffusion coefficient added. As mentioned in BGK, the effect of radiative transfer was not treated explicitly, although the zonal mean temperature was adjusted toward its initial value using a Newtonian-type damping with a 24-h damping period.

The average vertical profile of the relative humidity and temperature calculated for a 5° square region surrounding Hurricane Gloria on 1200 UTC 22 September 1985 served as the initial environmental condition of the mass and moisture fields for the idealized experiments presented in this study. In particular, the basic fields of temperature and relative humidity at each model level as well as the sea level pressure were computed by taking an average of these quantities from the National Center for Environmental Prediction (NCEP) T80 global analysis in the 5° square region centered on Hurricane Gloria. The SST was set to 302 K everywhere, which was the approximate value near the center of Hurricane Gloria at the initial time. This was the same initial condition used in BGK. The initial vertical profile of the environmental relative humidity and temperature is shown in Fig. 2a of BGK. The time of 1200 UTC 22 September 1985 was 18 h after Gloria was first upgraded to a hurricane and just prior to onset of rapid intensification. In the experiments that include easterly and westerly zonal flows, the initial zonal flows had constant angular velocities with respect to the earth's axis of rotation with zonal speeds of 5.0 m s⁻¹ at 18°N (initial latitude of the tropical cyclone center for each experiment). This resulted in a very weak latitudinal shear of about 30 cm s⁻¹ over a 1000-km distance centered on the storm. The zonal flows (identified as the basic flows) were constant with height, except for one experiment in which the magnitude of the basic flow gradually increased above the boundary layer to a value of about 16 m s⁻¹ at the upper levels.

Using the observed tangential wind profile for Gloria on 1200 UTC 22 September 1985, estimated from the official National Hurricane Center marine advisory valid at that time, the symmetric vortex was generated from a time integration of an axisymmetric version of the

TABLE 2. Summary of the idealized numerical experiments.

Direction of basic flow	Magnitude of initial basic flow (m s ⁻¹)	Experiment description
Assessment of effects of variation of Coriolis parameter (f):		
No basic flow	None	Constant f
No basic flow	None	Variable f
Assessment of effects of convective parameterization:		
		Variable f
No basic flow	None	No convective adjustment
Assessment of asymmetries with the addition of basic flows:		
Easterly	5	Constant f
Easterly	Vertical shear of 5–16	Constant f
Easterly	5	Variable f
Westerly	5	Variable f

hurricane model using the method outlined in section 4a of Kurihara et al. (1993). This symmetric vortex was then placed onto the basic flows (for the experiments with the easterly or westerly zonal flows) at 18°N. Following the procedure outlined in BGK, the mass field (temperature and sea level pressure) was recomputed through use of a static initialization method. The minimum sea level pressure of the model storm was 996 hPa at the start of the integration.

For the one real data case of Hurricane Gilbert, the initial field was obtained from the T80 analysis at 1200 UTC 14 September 1988. In this experiment the analyzed vortex was removed from the global analysis and replaced with a more realistic initial storm structure using the initialization scheme of Kurihara et al. (1993). The observed tangential wind profile was also estimated from the official National Hurricane Center marine advisory valid at the initial time.

b. Experimental design and summary of experiments

The outer domain of the model ranged from the equator to 55°N in the meridional direction for the idealized cases and from 10°S to 65°N for the case of Hurricane Gilbert. It remained fixed throughout the integrations, while the inner meshes of the tropical cyclone model moved with the storm center. All the experiments were integrated to 72 h, and the complete set of idealized experiments are summarized in Table 2. A set of experiments were run with no basic flow and either constant or variable Coriolis parameter (f). This second experiment (variable f) corresponded to the noncoupled experiment in BGK without a basic flow. One supplemental experiment was also performed without convective adjustment, in order to evaluate the sensitivity of the asymmetries observed in the variable f experiment to the convective parameterization. Two additional experiments were made with constant f to evaluate the asymmetries introduced by addition of a simple basic flow. First, an easterly basic flow of 5 m s⁻¹ was su-

perposed on the initial symmetric vortex. Next, an experiment was run with a simple easterly vertical shear in which the easterly flow steadily increased with height from 5 m s^{-1} above the boundary layer to a value of about 16 m s^{-1} at 10 km. To assess the impact of the addition of both the basic flows and the variation of f , two additional experiments were run with easterly or westerly basic flows and with variable f .

In each of the experiments run with constant f , the Coriolis parameter was set to the value at 18°N . Since the focus of this study is to examine the impact of the relative wind on the interior structure of the tropical cyclone, most of the analysis was performed for the interior portion of the finest mesh that had a horizontal resolution of $1/6^\circ$.

3. Definition of terms and discussion of the relative wind

The purpose of this section is to define some of the terms used in this study and to briefly discuss the storm's relative wind and the various quantities that will be emphasized throughout. For a vortex moving with propagation velocity \mathbf{C} (determined by computing the average displacement of the storm's center of mass), we define the relative wind \mathbf{V}_{rel} simply as the wind component computed with respect to a coordinate system moving with the storm. Namely,

$$\mathbf{V}_{\text{rel}} = \mathbf{V} - \mathbf{C}, \quad (3.1)$$

where \mathbf{V} is the velocity in the inertial frame.

Given a field, h , at any given moment of time (wind components, surface pressure, vorticity, divergence, precipitation rate, etc.), it can be split up into its symmetric (h_{sym}) and asymmetric (h_{asym}) components with respect to the storm center:

$$h = h(r)_{\text{sym}} + h_{\text{asym}}. \quad (3.2)$$

Here, the quantity $h(r)_{\text{sym}}$ is defined at each storm radius r as

$$h(r)_{\text{sym}} = \frac{1}{2\pi} \oint_0^{2\pi} h(r, \varphi) d\varphi, \quad (3.3)$$

where φ is the azimuthal angle.

The asymmetric component of the field h at any point is determined by subtracting the symmetric component $h(r)_{\text{sym}}$ from the total field h :

$$h_{\text{asym}} = h - h(r)_{\text{sym}}. \quad (3.4)$$

When the quantity h , which fluctuates with time, is averaged over a sufficiently long time period, a quasi-steady component \bar{h} can be determined. The instantaneous field h can then be written as the sum of \bar{h} and a transient component h' :

$$h = \bar{h} + h' = \bar{h}_{\text{sym}} + \bar{h}_{\text{asym}} + h'_{\text{sym}} + h'_{\text{asym}}. \quad (3.5)$$

The structure of \bar{h}_{asym} , that is, the quasi-steady asymmetric will be emphasized throughout the present study.

To determine the quasi-steady symmetric storm structure, various quantities for each time step were computed relative to the moving storm and time averaged for the final 36 h of integration. The primary features in the distribution of the various time-averaged quantities were found to be independent of the particular averaging interval as long as it was at least 24–36 h, which assured that the high-frequency asymmetries (i.e., h'_{asym}) were removed from the resulting fields. In the computation of the asymmetric wind field, the winds were first expressed in the cylindrical coordinate system. The asymmetric value was then obtained for both the radial and tangential flow by subtracting the symmetric part from both the tangential and radial component.

Since the relative flow moving across the vortex core will produce a strong asymmetric advective tendency as it enters the high-vorticity region of the interior, convergence and divergence may take place to counterbalance the above tendency. This suggests a probable relationship between the asymmetric relative wind and the asymmetric fields of convergence and divergence. Namely, asymmetric relative flow into the storm region should tend to be correlated with quasi-steady asymmetric convergence. Likewise, asymmetric relative flow out of the storm region should be associated with quasi-steady divergence. Since the vertical integral of convergence and divergence is related to upward motion and hence precipitation, the asymmetries in the quasi-steady distribution of convergence may well be related to asymmetries in the quasi-steady distribution of both upward motion and total storm precipitation. Clearly, this implies that the relative flow may be a major factor in the generation of asymmetries in the quasi-steady structure found in the interior of storms, as some of the observational studies have also suggested. In support of the above arguments, detailed analysis of the numerical results obtained in this study will first be made of the quasi-steady asymmetric structure of the divergence ($\bar{\nabla} \cdot \bar{\mathbf{v}}$)_{asym}, vertical motion ($\bar{\omega}$)_{asym}, and accumulated precipitation in the region of the eyewall, and second, of their relationship to the relative wind ($\mathbf{V}_{\text{asym}} - \mathbf{C}$).

4. Experimental results

In this section, the numerical results will be presented. In section 4a the quasi-steady symmetric vortex structure in the interior of the tropical cyclone will be shown for an experiment run with constant f and no basic flow. In section 4b the asymmetries in the tropical cyclone eyewall introduced by the variation of the earth's planetary vorticity with latitude will be examined. Evaluation of the effect of the asymmetric flow on the vorticity budget is the topic of section 4c. The effect of basic flows, both constant and increasing with height, on the storm asymmetries will be discussed in section 4d, and the effect of the relative wind on the generation of asymmetries for one real case of Hurricane Gilbert is described in section 4e.

a. Structure of a vortex with constant f and no basic flow

In the first experiment, a vortex with nearly constant intensity evolved with minimum sea level pressure reaching 935 hPa and maximum low-level winds of 54 m s⁻¹ at around 66 h. Although the surface pressure field of this storm was found to be nearly axisymmetric, the distributions of precipitation, convergence, and upward motion still tended to be dominated at any instant by high-frequency features such as cyclonically rotating convective cells in the eyewall region and bands of convergence and divergence propagating outward from the storm center. The 36-h averaging interval was found to be sufficient to smooth out these high-frequency asymmetries evident in the instantaneous fields. This time interval was also appropriate since during the final 36-h period the idealized storms in this study maintained a nearly steady state. For instance, in this first experiment the minimum sea level pressure and maximum low-level wind varied from 941 hPa to 935 hPa and from 51 to 54 m s⁻¹, respectively, during the 36-h period in which the time averaging was taken. In this first experiment, there were no significant factors that could cause a quasi-steady asymmetry to develop [\bar{h}_{asym} of (3.5)] except through small numerical inhomogeneities introduced into the solution. The vortex remained nearly stationary, with its location fluctuating only 20 km during the entire 72-h integration.

A northwest–southeast vertical cross section of divergence through the storm center (Fig. 1, top) shows that this quasi-steady storm structure was quite symmetric. To enhance the portion of the atmosphere near the surface, the vertical coordinate for these and all other cross sections is the square root of height in meters, where the vertical velocity component in this coordinate system is given by $d\sqrt{z}/dt$ so that $w = dz/dt = 2\sqrt{z}(d\sqrt{z}/dt)$. [See Fig. 11 of Bender et al. (1985) for more details of this coordinate system.] Maximum boundary layer convergence occurred in the eyewall region. The eyewall was characterized by strong upward motion extending from the boundary layer to the region of outflow that was located at around 14-km height. Strong divergence in excess of $2 \times 10^{-4} \text{ s}^{-1}$ was located in the outflow layer in the eyewall. Divergent flow was found in the lower part of the eye between 500 and 1500 m, which suggests outflow near the bottom of the eye. In the observational analysis of Frank (1984) for northward moving Hurricane Frederic (1979), maximum divergence at 560 m was found just to the west of the center of the eye with a weak divergent region extending to the south and east.

The accumulated precipitation distribution also appeared to be quite symmetric (Fig. 1, bottom), although some small spacial variations were still evident. However, when the locations of the strongest convective cells were sampled at 15-min intervals during the second half of the integration period, the positions of the maximum

precipitation within the eyewall were found to be nearly evenly divided between the four quadrants, with the maximum precipitation occurring 26%, 23%, 25%, and 26% of the time in the northwest, southeast, southwest, and northeast quadrants, respectively.

b. Asymmetries introduced by variation of f

In barotropic models with the variation of f included, a significant asymmetric wind is generated near the storm center, as the storm's cyclonic circulation produces a beta gyre by advection of lower (higher) planetary vorticity northward (southward) on the east (west) side of the storm. This results in vortex propagation basically in a northwest to north-northwest direction. For the present study with a multilevel model, the next experiment was carried out with the variation of the Coriolis parameter with latitude introduced. In this experiment, the tropical cyclone reached a maximum intensity with minimum sea level pressure of about 938 hPa and maximum low-level winds of 53 m s⁻¹, compared to 935 hPa and 54 m s⁻¹ for the experiment with constant f . The azimuthally averaged tangential wind in the lower part of the free atmosphere ($\sigma = 0.78$, ~ 2.1 km) is shown in Fig. 2 (top) averaged for the final 36-h interval and calculated with respect to the lower-level (i.e., $\sigma = 0.78$) circulation center. This approach and definition of the storm center was used throughout this study whenever the symmetric component of the various quantities was obtained. The radius of maximum wind was about 55 km ($\sim 0.5^\circ$) from the storm center, which is somewhat larger than observed for most storms of comparable intensity, due to the $1/6^\circ$ resolution that was still not able to fully resolve the interior structure of a more compact eyewall. The distribution of symmetric vorticity is shown (Fig. 2, bottom) for the interior region of the storm. From Fig. 2 (bottom), it is seen that the inner 120-km region, which is the primary focus of this study, was characterized by strong vorticity gradients. The impact of these strong gradients of vorticity on the generation of the quasi-steady asymmetries in the vorticity budget in this region will be demonstrated later.

Using a barotropic model, Fiorino and Elsberry (1989) have shown that a tangential wind profile in the outer storm region as in Fig. 2 will generate a significant asymmetric wind component. As mentioned in section 3, subtraction of the symmetric component from the total field determined the asymmetric distributions. In the present case, when the symmetric tangential wind profile (Fig. 2, top) was subtracted from the time-averaged total tangential wind, the resulting asymmetric wind distribution in Fig. 3 resulted. (The symmetric radial component at that model level was much smaller than the tangential component, and was neglected in the computation of this figure.) The relative vorticity distribution of the asymmetric flow exhibited a wavenumber 1 structure (not shown) with a relative vorticity minimum ($\sim -22 \times 10^{-6} \text{ s}^{-1}$) about 450 km northeast of

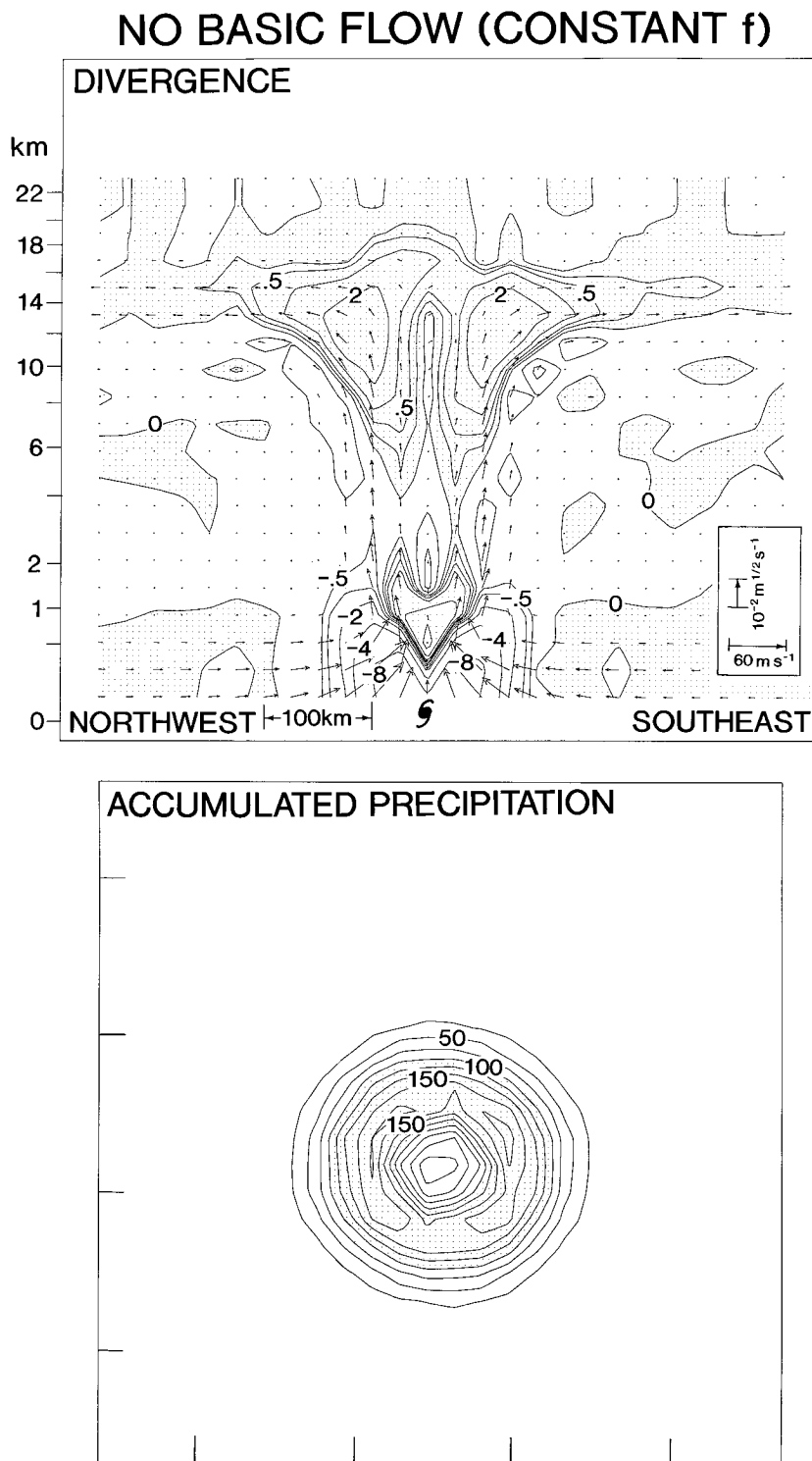


FIG. 1. For the constant f experiment, (top) northwest-southeast vertical cross section through the storm center of the radial-vertical flow field and the divergence (10^{-4} s^{-1}), computed from the wind field averaged for the final 36 h of the integration; and (bottom) the precipitation (cm) accumulated for the final 36 h of the integration and computed relative to the moving storm. The arrows indicate the radial-vertical motion. The hurricane center position is indicated by the hurricane symbol. The tick marks in the bottom panel are at 1° intervals. Regions of divergence and accumulated precipitation greater than 100 cm are lightly shaded.

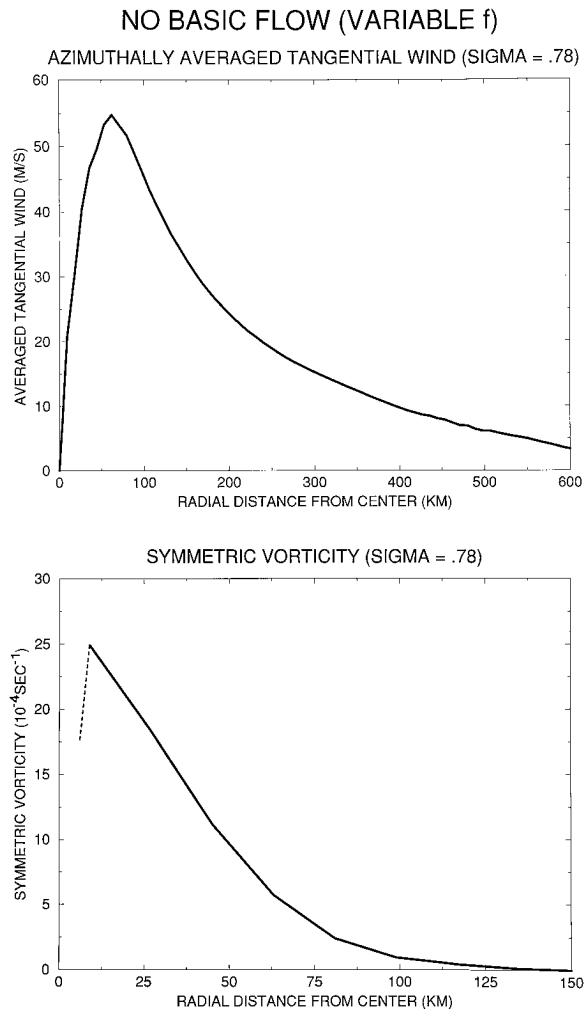


FIG. 2. For the experiment with variable f and no basic flow, the azimuthally averaged tangential wind (top, m s^{-1}) and symmetric vorticity (bottom, 10^{-4} s^{-1}) at model level $\sigma = 0.78$ ($\sim 2.1\text{-km}$ height), computed from the wind field averaged for the final 36 h of the integration. The dashed line indicates the region near the center where the vorticity cannot be accurately determined due to model resolution.

the storm center and a corresponding maximum of cyclonic vorticity ($\sim 20 \times 10^{-6} \text{ s}^{-1}$) approximately equal distance to the southwest. The general direction of the flow field in Fig. 3 was oriented in a north-northwest direction, in good agreement with the average direction of movement of the storm. As mentioned before, although the beta gyres were located in the outer region of the storm, they produced significant asymmetric flow into the inner region. The magnitude of the asymmetric flow field in the direction of the storm movement was computed next for different vertical levels by averaging it along a cross section in the direction of storm movement, passing through the storm center and stretching outward up to 250 km from the eye. In this computation, the values within 75 km of the storm center were excluded in order not to include the effects of the induced asymmetric circulation in the computation. It is pre-

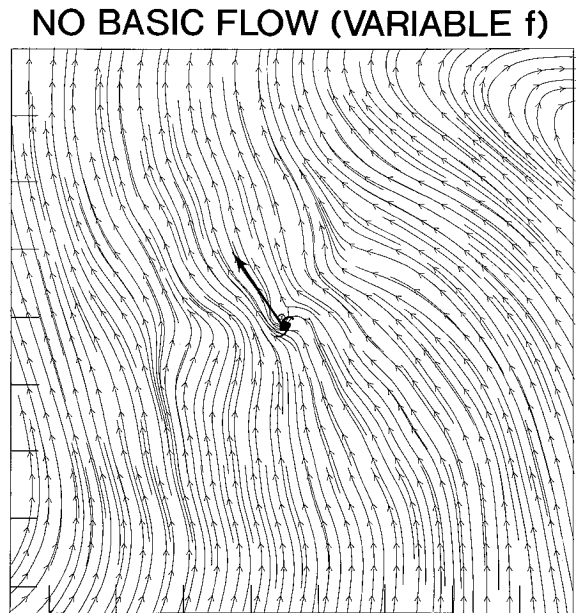


FIG. 3. Streamlines of the asymmetric wind field for the experiment with variable f and no basic flow at model level $\sigma = 0.78$ ($\sim 2.1\text{-km}$ height), computed from the wind field averaged for the final 36 h of integration. The region shown is for the entire inner nest, with the tick marks at 1° intervals. The storm direction is indicated by the thick arrow, and the hurricane center position is shown by the hurricane symbol.

sumed that this is a good representation of the asymmetric flow entering and leaving the interior region.

The vertical shear of the asymmetric flow in this experiment, which was oriented along the direction of the storm motion, was not directional but primarily due to changes in the magnitude with height. The component of the asymmetric wind in the direction of the storm movement (Fig. 4) was over 5 m s^{-1} in the lowest part of the free atmosphere and decreased with height to less than 2 m s^{-1} in the middle and upper troposphere. This vertical distribution was correlated with the strength of the tropical cyclone's cyclonic circulation, which was strongest just above the boundary layer and gradually decreased with height above this level. In this experiment, the storm basically moved with the speed of the vertically integrated asymmetric flow, that is, about 2.25 m s^{-1} (1.2 m s^{-1} westward and 1.9 m s^{-1} northward). Just above the boundary layer, the component of the relative wind exceeded the storm's translational speed by nearly 3 m s^{-1} , resulting in significant relative flow from the rear side of the storm into the eyewall. Relative flow into the storm from the south-southeast occurred from the boundary layer to slightly above 6 km.

The instantaneous distribution of convergence was characterized by bands of convergence and divergence that tended to propagate outward from the storm center. However, the general pattern of the time-averaged divergence and asymmetric divergence fields (Fig. 5) at level $\sigma = 0.78$ ($\sim 2.1 \text{ km}$), which was slightly above

ASYMMETRIC WIND COMPONENT IN DIRECTION OF STORM MOTION

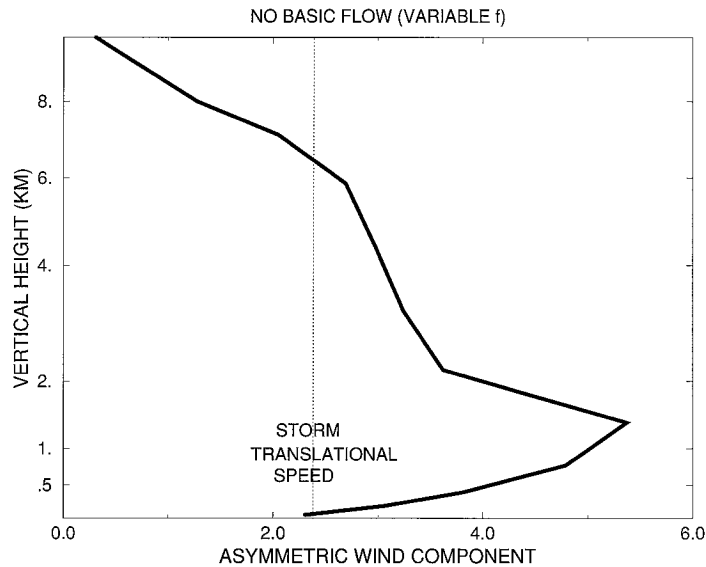


FIG. 4. Vertical profile of the 36-h averaged asymmetric wind component (m s^{-1}) in the direction of storm motion for the experiment with variable f and no basic flow. At each vertical level the average is taken along a cross section passing through the storm center. The mean translation speed of the storm ($\sim 2.2 \text{ m s}^{-1}$) is indicated by a dashed line.

the level of maximum relative flow, remained constant, indicating that it was produced by a persistent forcing mechanism. In the northwest (southeast) eyewall the averaged flow was predominantly divergent (convergent). Maximum value of total convergence and asymmetric convergence on the southeast side of the eyewall were both $-1.3 \times 10^{-4} \text{ s}^{-1}$, located about 60 km from the storm center. The time-averaged total divergence and asymmetric divergence on the northwest side had maximum values of $1.1 \times 10^{-4} \text{ s}^{-1}$ and $1.4 \times 10^{-4} \text{ s}^{-1}$, respectively, located 45 km from the storm center.

Vertical cross sections through the storm center in the direction of the storm motion for both the total divergence and asymmetric divergence are presented in Fig. 6, together with the radial-vertical flow field and the asymmetric relative wind and asymmetric vertical flow field that evolved for the experiment with variable f . The asymmetric divergence (Fig. 6, bottom) was largest (over $1.0 \times 10^{-4} \text{ s}^{-1}$) in the lower part of the free atmosphere, where the relative inflow and outflow across the vortex (Fig. 4; Fig. 6, bottom) was maximum. The asymmetric divergent (convergent) region in front (to the rear) of the eye extended from the boundary layer to the middle troposphere, similar to the vertical extent of where the relative flow was from the rear to the front. Consistent with the asymmetry in the convergence, the total upward motion (Fig. 6, top) was considerably stronger in the rear quadrant of the eyewall, compared to the front sector throughout the entire troposphere. Accordingly, the upper-level divergence in the outflow region in the variable f experiment was stronger to the rear of the storm center and weaker ahead of it.

In Fig. 7 the impact of the pattern of asymmetric convergence on the vertical motion (top) and accumulated precipitation (bottom) is shown. The averaged value of omega in the middle level of the atmosphere ($\sigma = 0.5$, $\sim 5.7 \text{ m}$) was nearly twice as large on the southeast side of the eyewall compared to the northwest quadrant. Similarly, the accumulated precipitation in the eyewall ranged from 100 cm ahead of the storm to 200 cm just to the rear of the storm center. The distribution of the accumulated precipitation was well correlated with the asymmetries in the convergence and the vertical velocity in the free atmosphere. The difference in precipitation between the constant f and variable f experiments was somewhat larger in the front of the eyewall ($\sim 75 \text{ cm}$) compared to the rear ($\sim 50 \text{ cm}$). Also, it was found that the decrease of upward motion at middle levels ahead of the storm between the variable f and the constant f experiments was greater than the increase of upward motion on the southeast side.

As shown in Fig. 8, the above-mentioned strongly asymmetric structure in the accumulated precipitation was masked in the instantaneous precipitation fields since this distribution was dominated by cyclonically rotating cells of precipitation within the eyewall. Although the strong convective cells (areas of maximum precipitation) were instantaneously located in any of the four quadrants, the most intense activity was often found in the southeast sector of the storm. This was a favored region for the intensification of the cells that often weakened considerably in the region northwest of the eye. In the present case, 70% of the occurrences of the heaviest precipitation in a sample taken at 15-min intervals

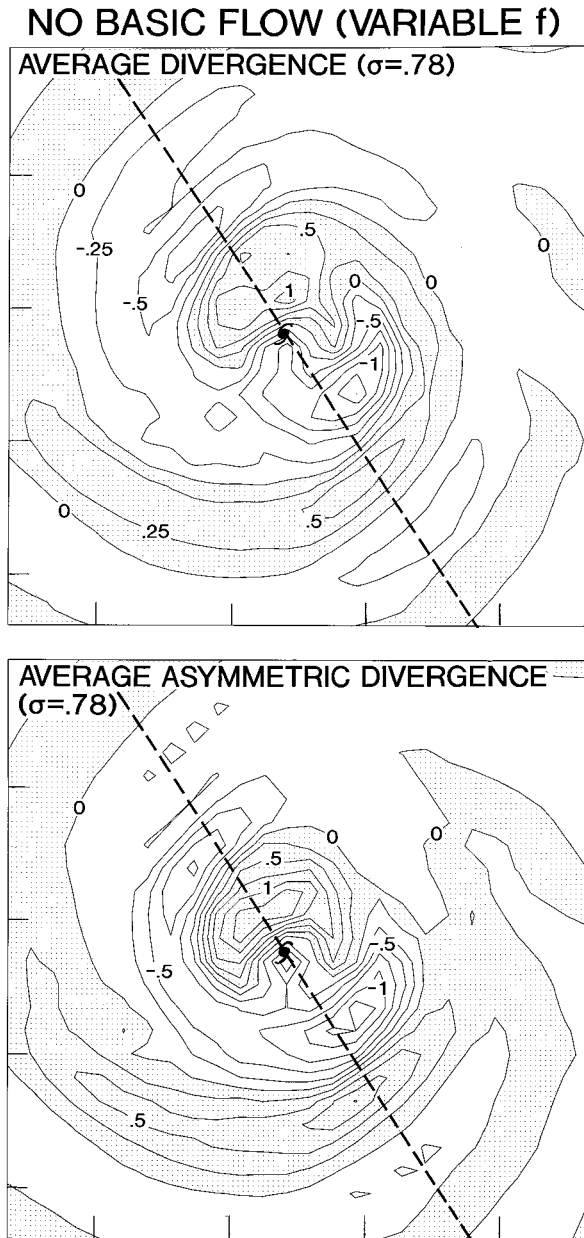


FIG. 5. Total divergence (top, 10^{-4} s^{-1}) and asymmetric divergence (bottom, 10^{-4} s^{-1}) for the variable f and no basic flow experiment at $\sigma = 0.78$ averaged for the final 36 h of the integration. The dashed line indicates the region through which the cross sections in Fig. 6 are taken. Regions of divergence are lightly shaded.

during the last 36 h of the integration period were found in the southeastern half of the vortex. When the domain was subdivided into four quadrants, the location of the maximum precipitation within the eyewall occurred in the northwest quadrant only 8% of the time, compared to 37% in the southeast quadrant and 28% and 27% in the southwest and northeast quadrants, respectively. Similar to the distribution of precipitation, the time-averaged maximum in upward motion on the southeast

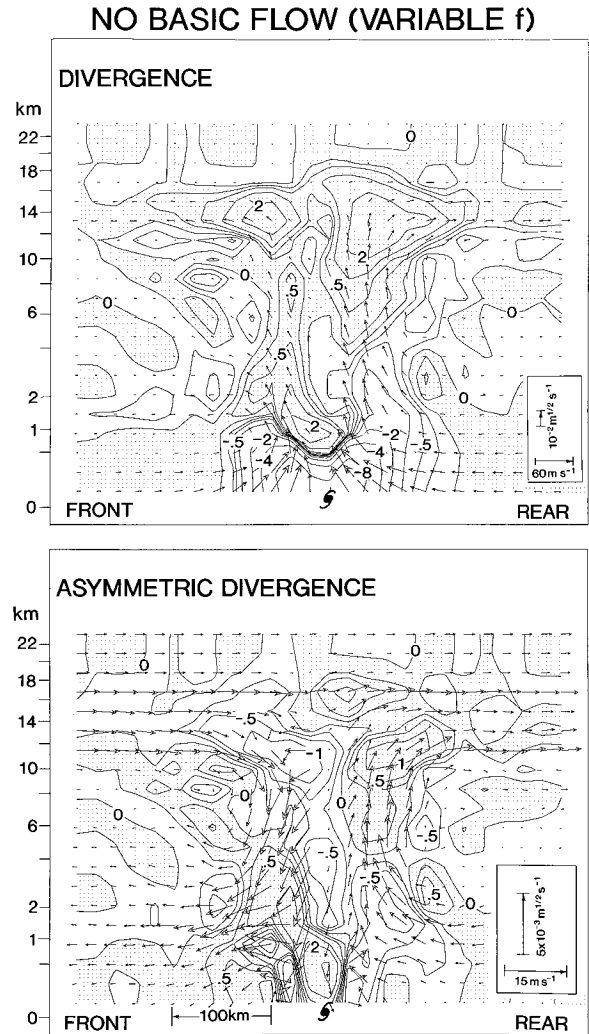


FIG. 6. Vertical cross sections through the storm center and in the direction of the storm motion for the radial-vertical flow field and the total divergence (top, 10^{-4} s^{-1}), and the asymmetric relative wind-asymmetric vertical flow field ($\bar{\mathbf{V}}_{\text{asym}} - \mathbf{C}, \bar{\mathbf{w}}_{\text{asym}}$) and asymmetric divergence (bottom, 10^{-4} s^{-1}), computed from the wind field averaged for the final 36 h of the integration for the experiment with variable f and no basic flow. See Fig. 1 for more details.

side of the eyewall was often masked in the instantaneous distributions of omega (not shown). The above analysis indicates that the greatest impact of the asymmetric flow on the precipitation was to reduce the magnitude of the strongest convection by the persistent area of divergence on the northwest side of the eyewall. This is likely one of the reasons the suppression of precipitation in front of the storm was somewhat larger than the enhancement behind the storm, between the constant f and variable f experiments. The large asymmetry between the front and rear quadrant, noted in the accumulated precipitation, was also likely enhanced by the correlation between precipitation and convergence once this asymmetry was generated in the baroclinic model.

Finally, to evaluate the possible role of the cumulus

NO BASIC FLOW (VARIABLE f)

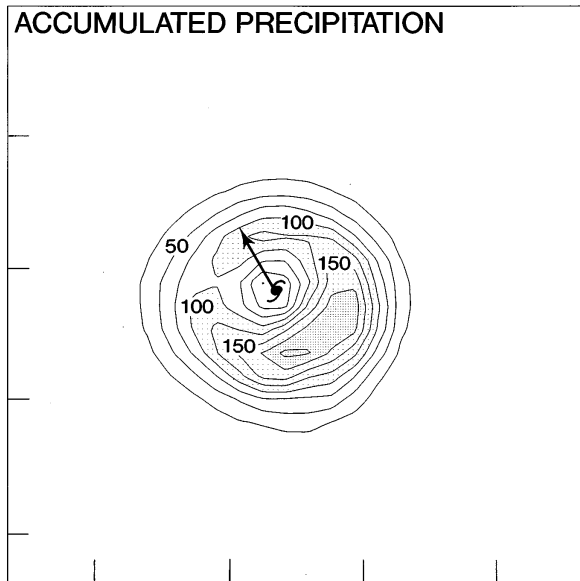
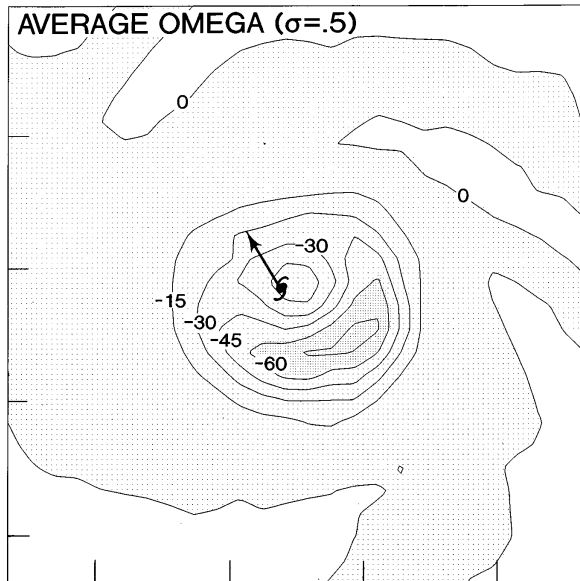


FIG. 7. Omega (top, 10^{-3} hPa s^{-1}) at $\sigma = 0.5$ (~ 5.7 -km height) and accumulated precipitation (bottom, cm) averaged or accumulated for the final 36 h of the integration and computed relative to the moving storm. Regions of negative values of omega (upward motion) or accumulated precipitation greater than 100 cm, are indicated with light shading. Regions with omega less than -60×10^{-3} hPa s^{-1} or regions where the accumulated precipitation exceeded 175 cm are shown by dark shading.

parameterization used in this study on the simulated storm asymmetry discussed above, a supplemental experiment was performed without cumulus parameterization. In this experiment, precipitation resulted only from the resolvable-scale processes. The numerical results indicated that the precipitation pattern (not shown) was quite similar to the asymmetric pattern

shown in Fig. 7 as the maximum precipitation remained on the southeast side of the eyewall. This suggests that the formation of the asymmetry in the precipitation discussed in this section was not due to the type of convective parameterization used. In other words, the precipitation in the present rather intense storm was largely dependent on the resolvable-scale vertical motion.

c. Evaluation of effect of relative flow on the vorticity budget

In the analysis of Hurricane Gert by Willoughby et al. (1984), it was suggested that as the environmental flow moved through the vortex core at the lower levels, it produced the pattern of convergence and divergence observed on the east and west side of the eyewall, through the mechanism of potential vorticity conservation. In particular, as the air entered the region of large vorticity gradients in the inner storm region, they proposed that vertical stretching occurred as the flow tended to conserve potential vorticity. Likewise, as the air exited on the west side, it was speculated that its vorticity was reduced by compression of the vortex tubes. It should be pointed out, however, that the potential vorticity will be greatly modified by the intense convective heating in the eyewall, which also tends to redistribute vertically the large potential vorticity found in the lower troposphere (e.g., Wu and Emanuel 1993), enabling the vorticity field to maintain its vertical coherence. Nevertheless, as discussed in section 3, a similar mechanism of vorticity forcing (i.e., vorticity stretching and compression) likely leads to the generation of the asymmetric distribution shown in Figs. 6 and 7. In order to investigate the effect of the strong vorticity forcing by the relative wind on the divergent-convergent pattern observed in the present experiment, a vorticity budget computation was made. In this analysis, four terms in the vorticity equation that represent interaction of the relative flow and the symmetric component of vorticity were computed with respect to the moving storm:

$$-(\bar{\mathbf{V}}_{\text{asym}} - \mathbf{C}) \cdot \nabla \bar{\zeta}_{\text{sym}} \quad (4.1)$$

(horizontal adv. of sym. vorticity by asym. rel. wind),

$$-(f + \bar{\zeta}_{\text{sym}}) \bar{\nabla} \cdot \bar{\mathbf{V}}_{\text{asym}} \quad (4.2)$$

(stretching by the asym. divergence),

$$-\frac{\partial \bar{\omega}_{\text{asym}}}{\partial x} \frac{\partial \bar{v}_{\text{sym}}}{\partial p} + \frac{\partial \bar{\omega}_{\text{asym}}}{\partial y} \frac{\partial \bar{u}_{\text{sym}}}{\partial p} \quad (4.3)$$

(tilting by asymmetric omega),

and

$$-\bar{\omega}_{\text{asym}} \frac{\partial \bar{\zeta}_{\text{sym}}}{\partial p} \quad (4.4)$$

(vertical advection of sym. vorticity by asym. omega).

(Here, ζ refers to relative vorticity.) There exist other

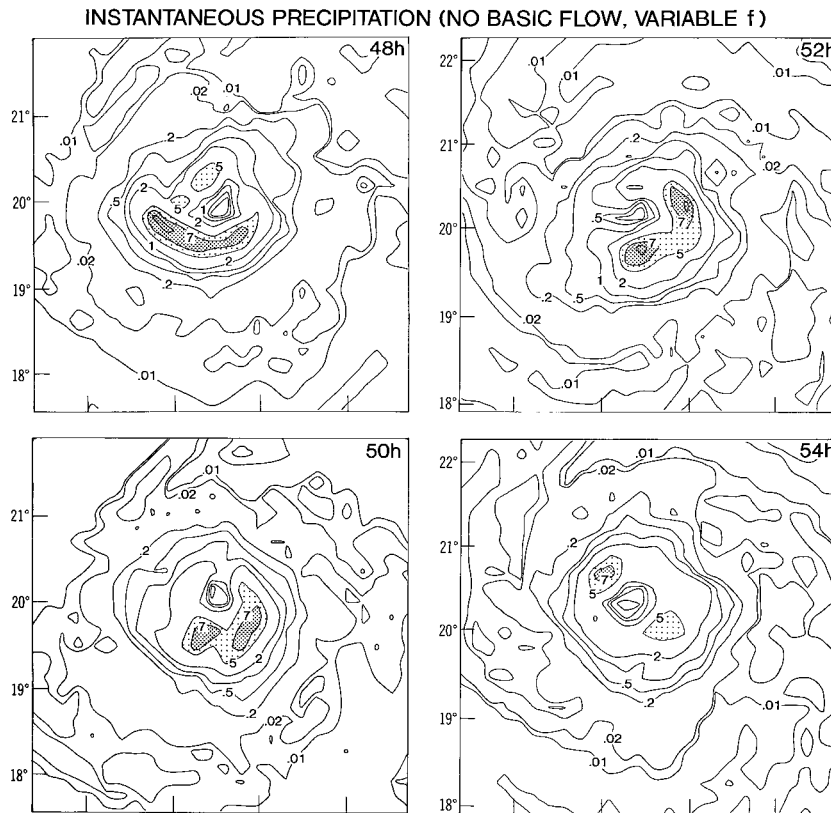


FIG. 8. Instantaneous precipitation rate (cm h^{-1}) at 48, 50, 52, and 54 h for the experiment with variable f and no basic flow. Contour intervals are drawn for 0.01, 0.02, 0.2, 0.5, 1, 2, 5, 7, and 9 cm h^{-1} . The regions with precipitation rates greater than 5 and 7 cm h^{-1} are indicated by light and dark shading, respectively.

terms involving the asymmetric vorticity and vertical derivatives of the asymmetric wind, namely

$$-\bar{\mathbf{V}}_{\text{sym}} \cdot \nabla \bar{\zeta}_{\text{asym}} - (f + \bar{\zeta}_{\text{asym}}) \bar{\nabla} \cdot \bar{\mathbf{V}}_{\text{sym}}$$

and

$$-\frac{\partial \bar{\omega}_{\text{sym}}}{\partial x} \frac{\partial \bar{v}_{\text{asym}}}{\partial p} + \frac{\partial \bar{\omega}_{\text{sym}}}{\partial y} \frac{\partial \bar{u}_{\text{asym}}}{\partial p} - \bar{\omega}_{\text{sym}} \frac{\partial \bar{\zeta}_{\text{asym}}}{\partial p}. \quad (4.5)$$

These terms were found to be significantly smaller than (4.1), (4.2), (4.3), and (4.4) in most of the regions of interest in this study. The horizontal distribution of the first two terms, (4.1) and (4.2), in the lower free atmosphere ($\sigma = 0.78$), are presented first (Fig. 9). This level was slightly above the region where the relative flow of the asymmetric wind $\bar{\mathbf{V}}_{\text{asym}} - \mathbf{C}$ was maximum. Although the relative flow at this level was $\sim 2 \text{ m s}^{-1}$, the large vorticity gradient in the eyewall region (Fig. 2, bottom) produced a vorticity tendency of $1\text{--}2 \times 10^{-7} \text{ s}^{-2}$ through the advection of the symmetric vorticity by the asymmetric relative flow (Fig. 9, top). The above distribution and magnitude was comparable to the stretching effect due to the asymmetric divergence (bottom). The magnitude of both terms was considerably larger in the front sector of the eyewall compared to the

rear. This feature was correlated with the larger decrease of accumulated precipitation in the front sector of the eyewall and the smaller increase of precipitation on the rear side between the variable and constant f experiments.

Vertical cross sections along the direction of storm motion for the terms (4.1), (4.2), (4.3), and (4.4) are presented in Fig. 10. Although the components of the asymmetric relative wind both in the direction of the storm and at right angles to the storm translation vector contributed to (4.1), the component in the direction of the storm motion was found to dominate in this experiment and was again plotted in the cross section for reference. In other cases, both components can make important contributions to this term. For example, as already pointed out, Franklin et al. (1993) found that the cross-track component of the relative environmental winds dominated in the interior of Hurricane Gloria. In Fig. 10, the contribution due to advection of symmetric vorticity by the relative flow was confined primarily to the eyewall region where the symmetric vorticity gradient was large. Note that, to first order, a good correlation was again found on both sides of the eyewall between the horizontal advection by the asymmetric

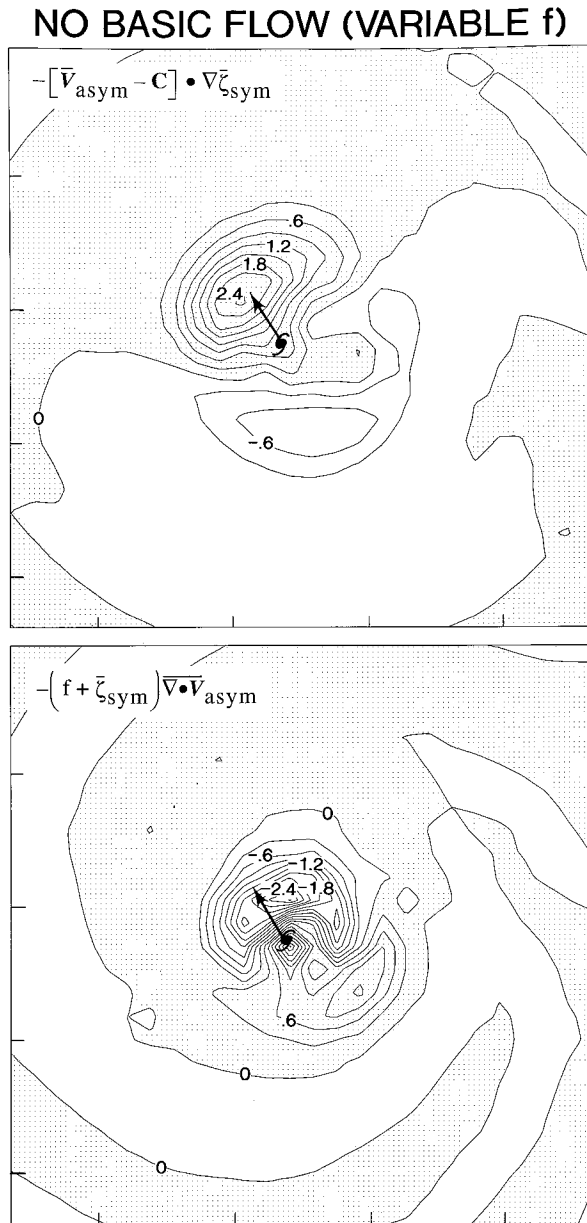


FIG. 9. The vorticity tendency (10^{-7} s^{-2}) defined by (4.1) (top, horizontal advection of symmetric vorticity by the asymmetric relative wind) and (4.2) (bottom, the stretching by the asymmetric divergence) for the variable f and no basic flow experiment at $\sigma = 0.78$ (~ 2.1 -km height) averaged for the final 36 h of the integration. The storm direction is indicated by the thick arrow, and the hurricane center position is indicated by the hurricane symbol. Positive values are indicated by light shading.

wind and the stretching effect by the asymmetric wind. Throughout most of the troposphere, both terms exhibited largest values ahead of the storm. Since the relative flow was from the front in the upper levels, the effect of the relative flow tended to enhance the stretching effect there.

The contribution from the vertical advection of sym-

metric vorticity (4.4) and the tilting term due to the asymmetric omega (4.3) was small above 0.5 km, although the tilting term made a small contribution in the upper boundary layer on the front and rear side of the eyewall. The vertical advection term also made a small impact in the outflow region of the inner eyewall. The balance of these four terms was not particularly good in the immediate eye region. Kurihara and Bender (1982) pointed out that the transient asymmetries play a significant role in the maintenance of the mean structure of the eye. In the region near the center, small changes in determination of the center position could also significantly affect calculation of the symmetric averaging. In addition, in the boundary layer the terms associated with the frictional effect will become important, as well in the vorticity balance.

In summary, in this second experiment with variable f , large asymmetries in the storm's interior resulted from the vertical shear of the beta-gyre flow (e.g., Fig. 4), which was primarily caused by the decrease of the storm's cyclonic circulation with height. As the storm propagated northwest with the vertically integrated beta-gyre flow, the storm moved more slowly than the asymmetric wind at the lower levels. This resulted in flow that moved through the vortex in the lower levels and produced a large value in the tendency for advection of the symmetric vorticity by the asymmetric wind (Figs. 9 and 10). To counterbalance this steady forcing, persistent areas of vorticity compression and stretching were produced ahead and behind the vortex, causing large asymmetries (e.g., Fig. 7) in the vertical velocity and accumulated precipitation.

d. Effect of basic flows in the generation of the storm asymmetries

The previous analysis in section 4b has demonstrated the effect that the relative flow had in producing important asymmetric characteristics in the storm structure. In reality, a tropical cyclone seldom exists in a quiescent environment, but rather in environments associated with large changes in the large-scale flow, both in the horizontal and vertical. These vertical changes in the environmental flow will cause large vertical variation in the relative flow. For example, in Hurricane Gloria, Franklin et al. (1993) observed that the asymmetric relative wind at 200 hPa was almost a complete mirror image of the 850-hPa flow pattern. From the previous results we can speculate that these large vertical changes will likely impact the generation of asymmetries in the interior region.

The purpose of the present section is to demonstrate this effect with simple basic flows. The basic flows in the first two experiments at the initial time were an easterly flow that was constant with height and an easterly basic flow with vertical shear. Since it has already been shown (Fig. 1) that without the basic flow the quasi-steady state of the vortex in the experiment with

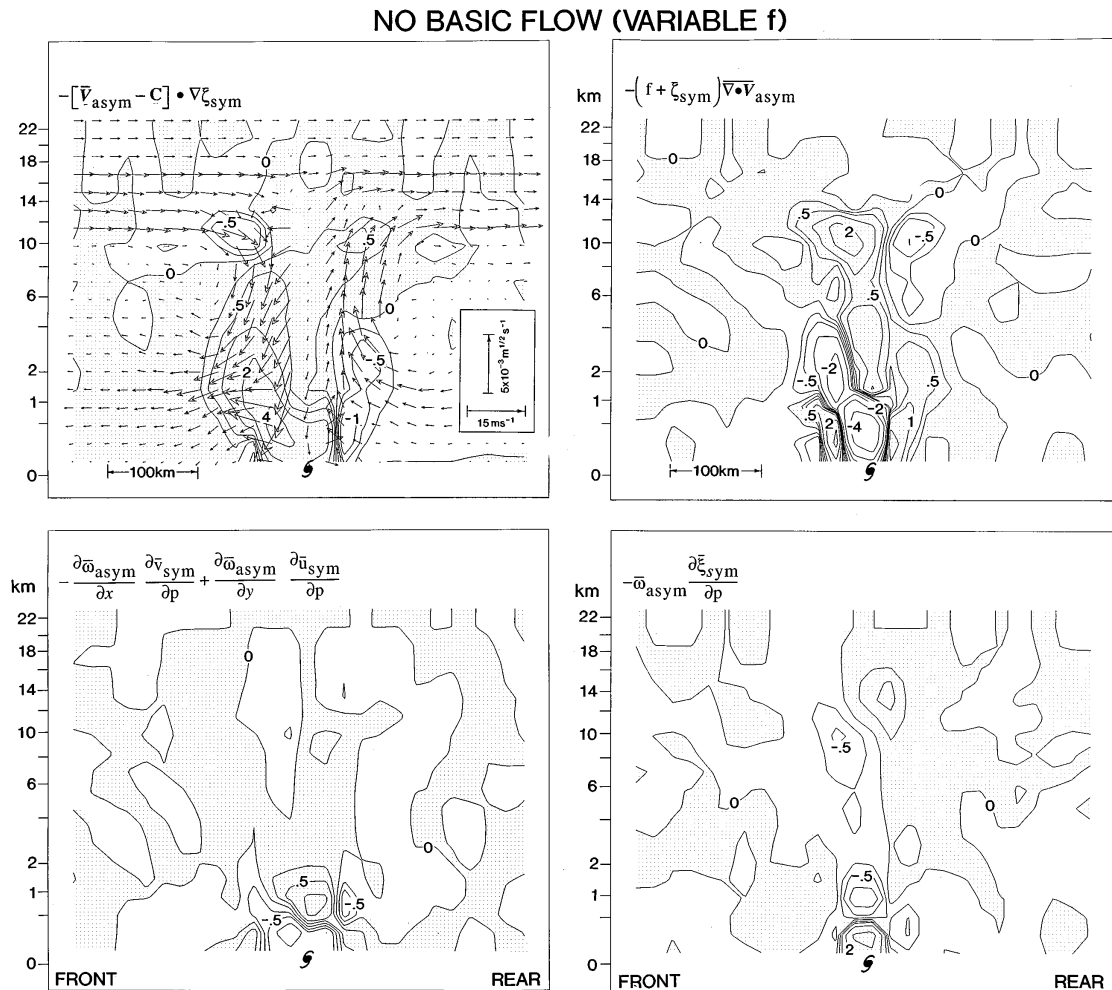


FIG. 10. Vertical cross sections through the storm center and in the direction of the storm motion for the vorticity tendency terms ($10^{-7}, \text{s}^{-2}$) defined by (4.1) through (4.4) for the variable f and no basic flow experiment computed from the wind field averaged for the final 36 h of the integration. The wind vectors plotted show the flow field for the asymmetric relative and vertical wind ($\bar{\mathbf{V}}_{\text{asym}} - \mathbf{C}, \bar{\mathbf{w}}_{\text{asym}}$). The storm center is indicated by the hurricane symbol, and positive values are indicated by light shading. See Fig. 1 for more details.

constant f was almost perfectly symmetric, these two experiments were first run with constant f in order to isolate the effect of the basic flow on the vortex.

The asymmetries introduced by the initially constant easterly basic flow of 5 m s^{-1} are discussed first (Fig. 11, left). In this experiment, the storm moved west with no north or south drift at 4.9 m s^{-1} . In the boundary layer the relative flow was from the front to the rear. As shown by Shapiro (1983) and Chow (1971), a translating vortex with a constant basic flow will exhibit increased convergence in the boundary layer ahead and just to the right of the moving vortex, associated with the region of maximum inflow. Shapiro (1983) speculated that this effect may contribute to larger values of accumulated precipitation in the front sector of moving storms, which have been observed in many observational studies (e.g., Marks 1985; Burpee and Black 1989). In results presented here, the asymmetry in the

boundary layer convergence is evident in Fig. 11 both in the distribution of total divergence (left, top) and asymmetric divergence (left, middle), as the latter quantity in the eyewall averaged about $-2 \times 10^{-4} \text{ s}^{-1}$ in the front boundary layer of the storm and $0.5\text{--}1.0 \times 10^{-4} \text{ s}^{-1}$ to the rear.

As clearly seen in Fig. 11 (left, middle), a maximum in the zonal wind component also occurred just above the top of the boundary layer, centered at 1.5 km ($\sim 850 \text{ hPa}$). This apparently resulted from the interaction of the basic flow with the vortex, since the increase of the zonal wind was not observed in the regions well beyond the storm region. This feature also tended to increase as the distance from the vortex center decreased. For example, the difference in the zonal wind measured between 500 and 850 hPa averaged only about 0.30 m s^{-1} 300 km from the storm center, increasing to 2 m s^{-1} within 200 km from the center, with a difference of 4.5

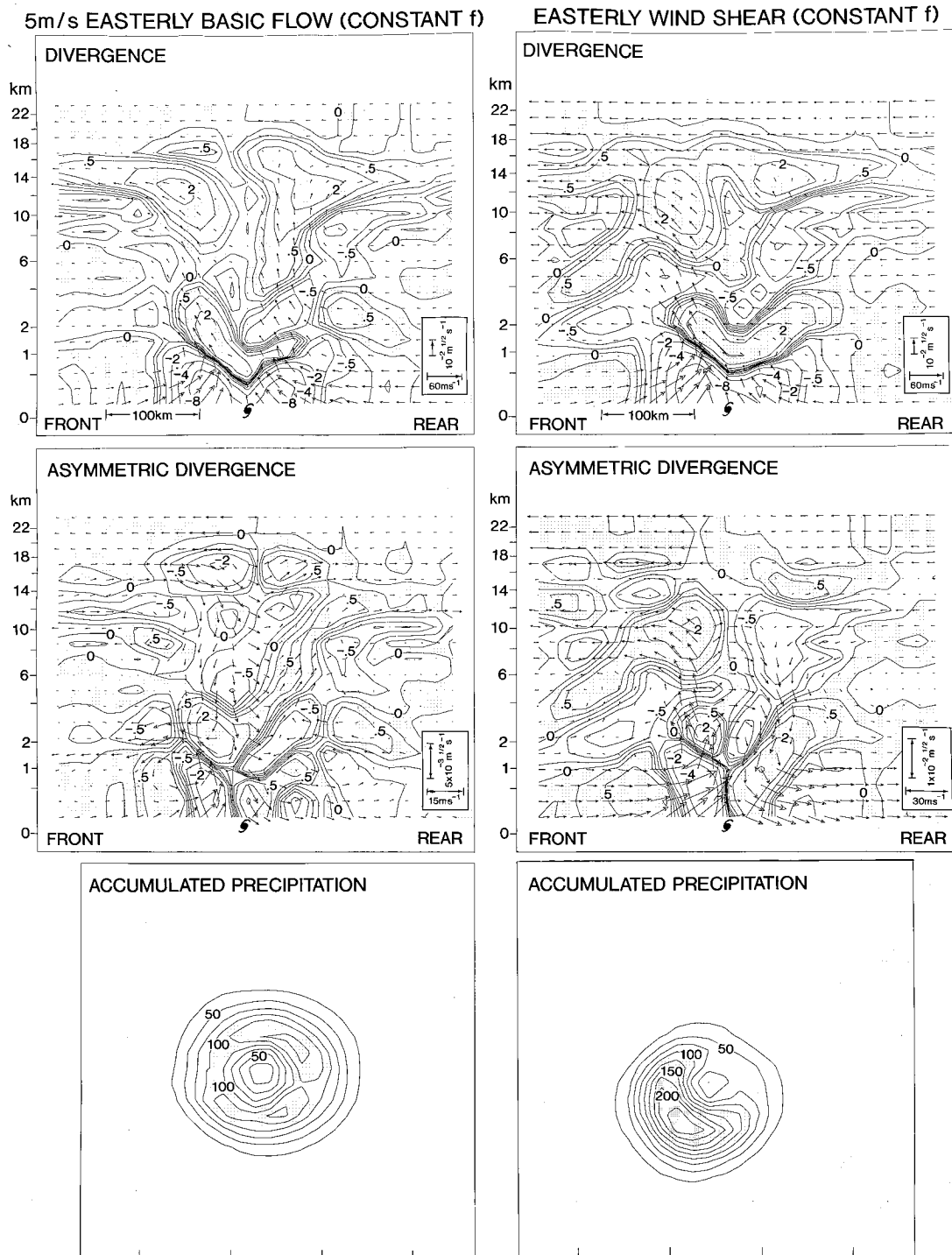


FIG. 11. Vertical cross sections through the storm center and in the direction of storm motion for the 36-h averaged radial-vertical flow field and total divergence (top, 10^{-4} s^{-1}), the asymmetric relative wind-asymmetric vertical flow field ($\bar{\mathbf{V}}_{\text{asym}} - \mathbf{C}, \bar{\mathbf{w}}_{\text{asym}}$) and asymmetric divergence (middle, 10^{-4} s^{-1}), and the distribution of the 36-h accumulated precipitation (bottom, cm) for the experiment run with 5 m s^{-1} easterly basic flow and constant f (left) and easterly wind shear and constant f (right). Regions of positive values of divergence or asymmetric divergence, and accumulated precipitation greater than 100 cm are indicated with light shading. Areas of accumulated precipitation greater than 175 cm are indicated with thick shading. See Fig. 1 for more details.

ASYMMETRIC WIND COMPONENT IN DIRECTION OF STORM MOTION

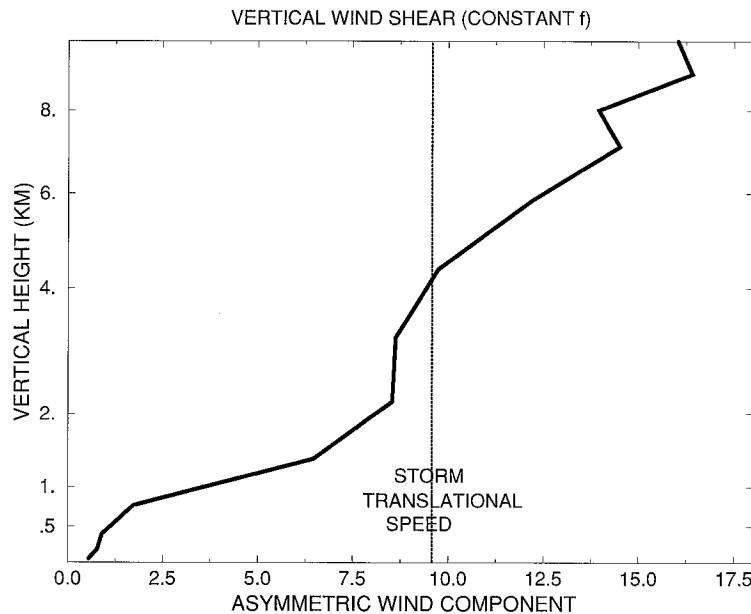


FIG. 12. Vertical profile of the 36-h averaged asymmetric wind component (m s^{-1}) in the direction of storm motion for the experiment with easterly vertical wind shear and constant f . The mean translation speed of the storm ($\sim 9.7 \text{ m s}^{-1}$) is indicated by a dashed line. See Fig. 4 for more details.

m s^{-1} 125 km from the storm center. It is speculated that this interaction of the basic flow and the vortex may be primarily forced from the boundary layer beneath and is a topic that will warrant further investigation in the future. Nevertheless, it resulted in relative flow between 1 and 3 km, which moved through the vortex from the rear to the front of the storm and produced a region of asymmetric divergence ahead and asymmetric convergence behind the storm (Fig. 11, middle left) in the lower part of the free atmosphere. This divergent-convergent pattern in the lower free atmosphere, which was opposite in sign to the asymmetric pattern found in the boundary layer, had much more of a significant impact in the upward motion in the eyewall than the asymmetries in the boundary layer convergence underneath. As a result, the accumulated precipitation exhibited a small increase ($\sim 35 \text{ cm}$) to the rear of the storm compared with the front side (Fig. 11, bottom left).

In the vertical shear experiment, the easterly basic flow was increased from 5 m s^{-1} at 1.5 km to 16 m s^{-1} at 10 km. Figure 12 shows the vertical distribution of the asymmetric flow during the final 36 h of integration, averaged for the regions in front and to the rear of the eyewall. The component of the wind in the boundary layer was considerably smaller ($\sim 5\text{--}9 \text{ m s}^{-1}$ less) than the storm translational speed, and the relative wind ahead of the storm was from the front side below 4 km. Above 5 km, there was strong relative flow from the rear toward the center of the storm. In the outflow layer

in the upper levels the asymmetric wind was $5\text{--}7 \text{ m s}^{-1}$ greater than the storm's translational speed.

The impact of this distribution of the relative flow on the divergence, upward motion, and precipitation is demonstrated on the right side of Fig. 11. In this experiment with vertical shear, the asymmetric divergence was greatly impacted by the relative flow in both the lower and upper levels. The average boundary layer asymmetric convergence (divergence) ahead (behind) the storm increased from about $-2 \times 10^{-4} \text{ s}^{-1}$ ($0.5\text{--}1 \times 10^{-4} \text{ s}^{-1}$) in the constant basic flow experiment to values of over $-4 \times 10^{-4} \text{ s}^{-1}$ ($2\text{--}4 \times 10^{-4} \text{ s}^{-1}$) in the case with easterly shear (Fig. 11, right, middle). Also note the region of total divergence and asymmetric divergent flow in the rear of the storm in the shear case, extending into the lower free atmosphere between 1 km and 4 km. Its vertical extent was well correlated with where the relative flow was from the front to the rear. Likewise, the region of upper-level divergence in the easterly shear case was considerably larger in front of the storm compared to the rear side. As a result, the upward motion became much more asymmetric between the front and rear eyewall. Consistent with much stronger upward motion in the front of the storm (right, top), the precipitation maximum shifted to the front sector of the storm. The accumulated precipitation was larger in the front left eyewall compared to the front right quadrant (right, bottom). This may be a result of tilting of the vertical axis of the vortex in the direction of the

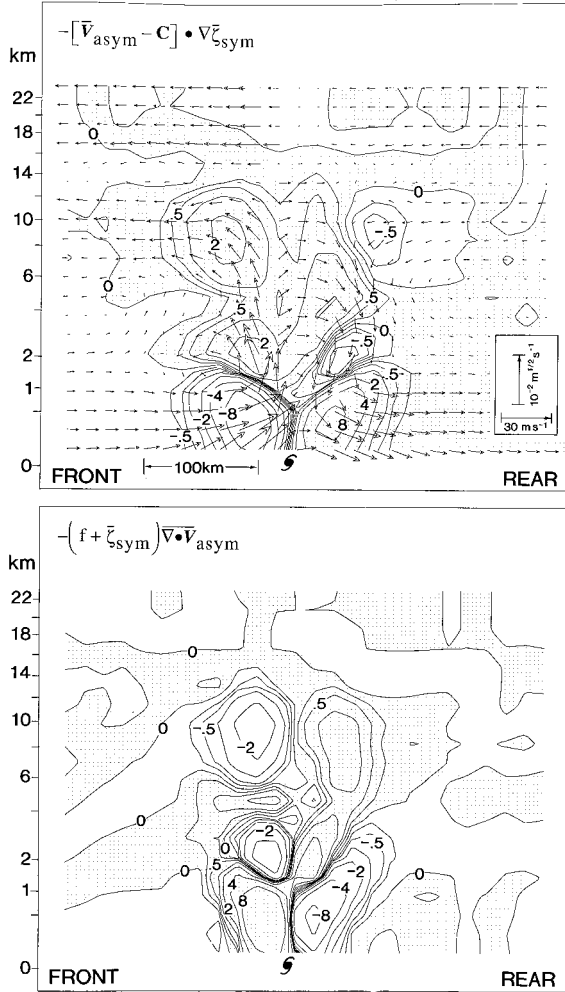
EASTERLY WIND SHEAR (CONSTANT f)

FIG. 13. Vertical cross sections through the storm center and in the direction of storm motion for the vorticity tendency terms (10^{-7} , s^{-2}) defined by (4.1) (top, horizontal advection of symmetric vorticity by the asymmetric relative wind) and (4.2) (bottom, the stretching by the asymmetric divergence) for the experiment with easterly vertical wind shear and constant f . The wind vectors plotted show the flow field for the asymmetric relative and vertical wind ($\bar{\mathbf{V}}_{\text{asym}} - \mathbf{C}$, $\bar{\mathbf{w}}_{\text{asym}}$). The storm center is indicated by the hurricane symbol, and positive values are indicated by light shading. See Fig. 1 for more details.

shear vector. This increased the horizontal vorticity in the direction of the shear vector (toward the west in the present case), and enhanced the vertical motion in the region to the left of the shear vector and decreased it to the right of the shear vector.

To quantitatively assess contributions of the relative wind on the vorticity budget for the case with easterly shear, the terms of horizontal vorticity advection by the asymmetric relative wind (4.1) and asymmetric stretching (4.2) were again calculated. From Fig. 13 it is seen that the two terms were well correlated, both in the boundary layer, in the lower part of the free atmosphere, and at the level of divergent outflow. In the boundary

layer, the strong relative flow from the front to the rear caused large vorticity stretching ahead and vorticity compression to the rear of the vortex. Likewise, in the outflow layer in the upper levels where the relative wind acted in the opposite direction, both terms reversed signs, and the divergent outflow was significantly increased on the front side of the storm and reduced to the rear. Combination of the two effects, that is, modification of the boundary layer convergence and upper-level divergence, served to increase the upward motion ahead of the translating vortex and decrease it in the rear quadrant of the eyewall, and contributed to the asymmetry in the distribution of accumulated precipitation.

Many of the observed studies have shown that the front sector of propagating tropical cyclones is often found to be a favored region of maximum rainfall, although the precipitation patterns are found to be highly variable from one storm to the other or even one time level to another (e.g., Marks et al. 1992). In a previous numerical simulation of Hurricane Gloria (1985) by the Geophysical Fluid Dynamics Laboratory (GFDL) model (Kurihara et al. 1990), a pronounced asymmetry in the precipitation pattern was obtained as the model storm accelerated north with heaviest precipitation occurring well ahead of the storm center and little precipitation south of the eye. This result agreed well with observed radar pictures presented in Franklin et al. (1988). During the period that the asymmetric precipitation pattern developed, strong southerly vertical wind shear existed in the region near the storm as the mean wind surrounding the hurricane increased from about 6 m s^{-1} at 850 hPa to nearly 23 m s^{-1} at 250 hPa. Analysis of the asymmetric pattern that was simulated by the GFDL hurricane model for one case of Hurricane Gilbert (1988) will be presented in the next section. These numerical results from real cases strongly support those of the idealized experiments, that is, that the vertical shear of the asymmetric wind and the resulting relative wind across the vortex may be one of the primary mechanisms that determine the quasi-steady asymmetric distribution of precipitation in tropical cyclones.

Recent studies by Shapiro (1992), Wu and Emanuel (1993), and Wu and Emanuel (1994) discussed effects of the vertical shear of the basic flow and the potential vorticity (PV) gradient on the storm structure and motion. The propagation of a vortex in a baroclinic environment is related to the gradient of the PV in a manner similar to a barotropic vortex on a beta plane. For the case of easterly shear and constant f presented here, the background PV gradient at 72 h in the north-south direction was about 0.03 PVU (potential vorticity units) $(1000 \text{ km})^{-1}$, estimated by taking the average difference between PV at 500 km north and 500 km south of the storm and averaging it for the isentropic surfaces between 320 and 330 K. This was about one-fifth of the PV gradient attributable to the variation of f that was absent in the present experiment. Consistent with this

ASYMMETRIC WIND COMPONENT IN DIRECTION OF STORM MOTION
5 M/S EASTERLY BASIC FLOW (VARIABLE f)

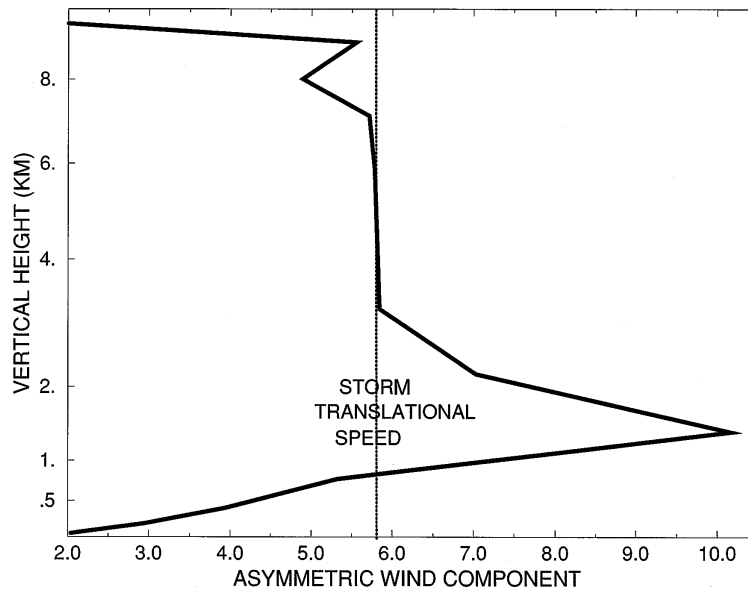


FIG. 14. Vertical profile of the 36-h averaged asymmetric wind component (m s^{-1}) in the direction of storm motion for the experiment with 5 m s^{-1} easterly flow and variable f . The mean translational speed of the storm ($\sim 5.8 \text{ m s}^{-1}$) is indicated by a dashed line. See Fig. 4 for more details.

weak PV gradient, the storm exhibited only a very small southward motion of about 40 cm s^{-1} . These results suggest that the background gradient of PV associated with the vertical shear chosen here did not have a significant impact on the storm structure.

In the last set of idealized experiments, the model was run with initially constant easterly or westerly basic flows of 5 m s^{-1} and with variable f . The vertical distribution of the asymmetric wind component in the direction of storm motion that evolved in the case of variable f and 5 m s^{-1} easterly basic flow is shown in Fig. 14. The obtained profile was somewhat similar to the sum of the vertical distribution for the case of no basic flow and variable f (Fig. 4) and that for the case of constant easterly basic flow and constant f (not shown). Relative flow into the storm from the rear side extended from the upper boundary layer to 3 km with a maximum value of over 4 m s^{-1} at 850 hPa ($\sim 1.5 \text{ km}$). The previous analysis suggests that this should have a significant impact on the asymmetric distribution of divergence and upward motion. The boundary layer convergence and accumulated precipitation are presented in Fig. 15 for cases both with easterly and with westerly constant basic flows and variable f . Similar to the case with variable f and no basic flow (Fig. 7), the precipitation maximum was located in the southeast sector of the storm for both experiments (Fig. 15, bottom), despite the maximum asymmetry in the boundary layer convergence ahead of the moving storm (Fig. 15, top) where the relative inflow was largest. This indicates that the

relative wind associated with the beta gyre became the primary mechanism producing the asymmetries in the precipitation and omega field in the absence of the large initial easterly vertical shear. The asymmetry in the boundary layer divergence for both the easterly and westerly basic flows (Fig. 15, top) again did not make a significant contribution to the asymmetry in the accumulated precipitation. In vertical cross sections of divergence through the storm center (not shown), the asymmetries in the divergence field for the variable f case indeed became larger in both the lower part of the free atmosphere and the upper levels compared to the constant easterly and constant f experiment. Hence, the upward motion became somewhat weaker ahead of the storm and slightly stronger in the rear eyewall.

e. Asymmetries in the eyewall of Hurricane Gilbert (1988)

In the last experiment, the model integration and analysis procedure used in the previous idealized experiments were applied to one real case of Hurricane Gilbert (1988). This particular case was selected since Hurricane Gilbert moved in a nearly constant west-northwest direction at a similar translational speed and direction as the 5 m s^{-1} easterly flow case with variable f . The initial condition, experimental design, and lateral boundary condition were identical to those described in Bender et al. (1993b). This integration was a 72-h forecast with the initial field obtained from the NCEP T80

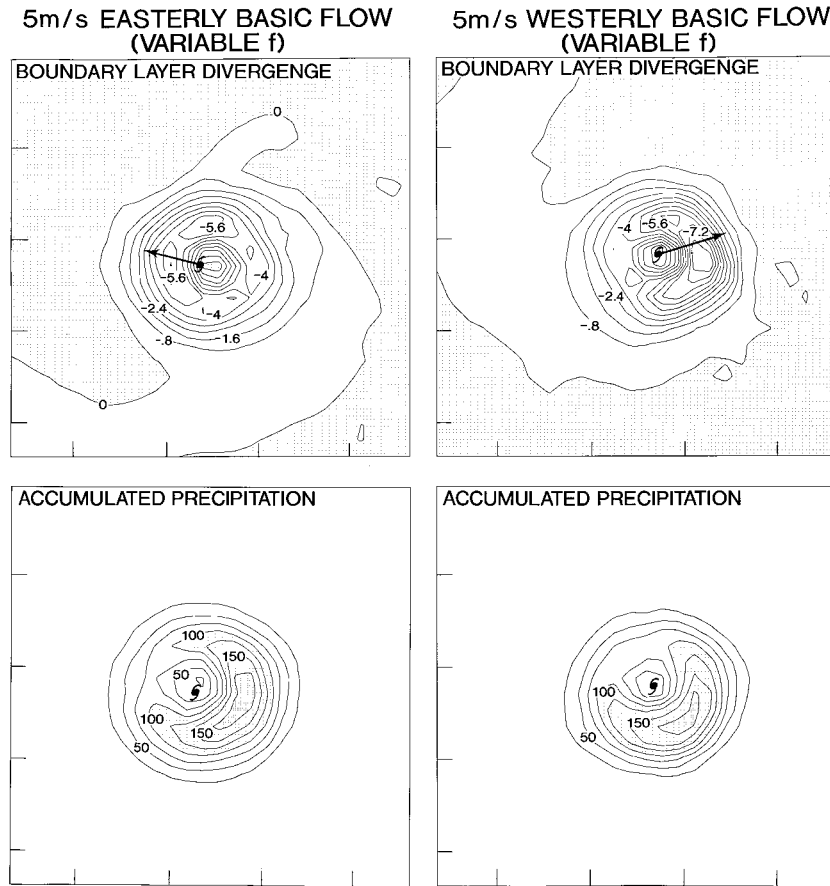


FIG. 15. The distribution of the boundary layer divergence (top, 10^{-4} s^{-1} , integrated from the surface to $\sigma = 0.89$, $\sim 1.1 \text{ km}$) and accumulated precipitation (bottom, cm) for the variable f experiments run with 5 m s^{-1} easterly and westerly initial basic flows. All of these were averaged or accumulated for the final 36 h of the integration and computed relative to the moving storm. Regions of divergence and accumulated precipitation greater than 100 cm are shaded. Areas of accumulated precipitation greater than 175 cm are indicated with thick shading. The storm direction is indicated in the upper panels by the thick arrow.

analysis at 1200 UTC 14 September 1988, just prior to the landfall of the hurricane on the Yucatan peninsula. Since the analyzed vortex was removed from the global analysis and replaced with a more realistic storm structure that was derived from the observed storm profile, it is assumed that the model storm during the integration resembled Hurricane Gilbert, at least to a first order. Similar to the previous experiments, a 36-h averaging interval was used, commencing at forecast hour 12, when the hurricane had moved again over water after emerging into the Gulf of Mexico. The averaging period ended about 12 h before the storm made landfall again over Mexico, so that the effect of land on the hurricane structure should have been minimal. Although Hurricane Gilbert changed little in intensity during this time, the model storm underwent moderate strengthening, with the minimum pressure decreasing from 952 to 940 hPa and the maximum low-level winds increasing from 39 to about 49 m s^{-1} . It is unclear the effect this had in changes in storm structure and on the generation of

the quasi-steady storm asymmetries. In addition, other factors such as horizontal variations in the wind fields may also have impacted the generation of the observed asymmetries. Nevertheless, analysis of this case should help to quantitatively verify the results that were derived from the previous analysis on the effect of the relative flow on the idealized storms.

Analysis of the 36-h average environmental wind indicated relative flow moving through the vortex generally from west to east, from the middle boundary layer where it was maximum, gradually decreasing with height to about 10 km. Hence the environmental wind exhibited easterly wind shear that resembled the vertical profile for the previous idealized experiment with constant f and easterly wind shear (e.g., Fig. 12), although it was considerably less in magnitude. The resulting vertical profile of the time-averaged asymmetric relative flow, computed in the direction of the storm motion, is shown in Fig. 16. During this time the model hurricane moved at 5.4 m s^{-1} in a west-northwest direction (e.g.,

ASYMMETRIC WIND COMPONENT IN DIRECTION OF STORM MOTION
HURRICANE GILBERT (1988)

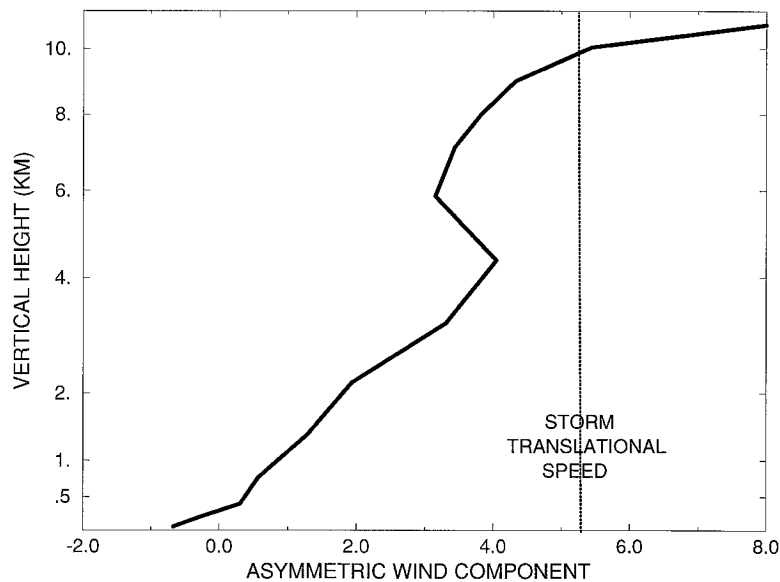


FIG. 16. Vertical profile of the 36-h averaged asymmetric wind component (m s^{-1}) in the direction of storm motion for the case of Hurricane Gilbert (1988). The mean translational speed of the storm ($\sim 5.4 \text{ m s}^{-1}$) is indicated by a dashed line. See Fig. 4 for more details.

4.9 m s^{-1} west and 2.2 m s^{-1} north). The resulting relative flow averaged about 6 m s^{-1} into the storm from the front in the boundary layer and $1\text{--}4 \text{ m s}^{-1}$ in the free atmosphere. In the vorticity budget, the term of the horizontal advection of symmetric vorticity by the asymmetric flow (not shown) was positive (negative) throughout much of the troposphere to the rear (in front) of the storm and in the region of large vorticity gradient, with maximum in the boundary layer ranging between 1×10^{-7} to $2 \times 10^{-7} \text{ s}^{-2}$ to the rear and from -0.5×10^{-7} to about $-1 \times 10^{-7} \text{ s}^{-2}$ in the front quadrant. The effect of stretching by the asymmetric divergence tended to counteract the advection effect. For example, this term in the rear eyewall was negative with a similar magnitude ($\sim -0.5 \times 10^{-7} \text{ s}^{-2}$) as the advection term from about 3 km to the outflow layer.

The structure of the total divergence and asymmetric divergent field is shown in Fig. 17. During this period the inner structure of the hurricane was rather broad with an average radius of maximum wind of about 110 km. Associated with the relative flow into the storm at low levels in the front quadrant of the eyewall, a region of asymmetric convergence (vorticity stretching) was found throughout the boundary layer to about 3 km, tilting to the west with height and extending to nearly 200 km from the storm center. This resulted in a large region of boundary layer convergence in the front of the eyewall (Fig. 17, top). In the rear eyewall where the relative flow out of the eyewall was occurring throughout much of the free atmosphere, the flow was divergent from about 3 km to the outflow layer above.

Corresponding to the asymmetric divergent distribution, the upward motion became distinctly stronger on the front side of the eyewall (Fig. 17, top). A highly asymmetric distribution in the accumulated precipitation (Fig. 17, bottom) resulted with the maximum precipitation found in the left front quadrant. The maximum accumulated precipitation between the southwest and northeast quadrant varied from 125 to 50 cm, and the asymmetric precipitation pattern was very similar to the previous idealized experiment with easterly shear (Fig. 11, right bottom). The agreement shown here provides strong support to the validity of the idealized experiments and to the present real case study as well.

5. Summary and discussion

Some of the previous analyses of observed hurricanes (e.g., Willoughby et al. 1984; Marks et al. 1992; Franklin et al. 1993) have strongly suggested that the vertical shear in the environmental flow and the resulting relative wind across the vortex, is one of the primary mechanisms in the generation of asymmetries in the convection found in the interior of tropical cyclones. A series of experiments were performed using the GFDL high-resolution hurricane model to investigate the effect of the asymmetric relative flow on the generation of asymmetries within the region of the eyewall. The quasi-steady component was emphasized, calculated by averaging the wind, divergence, omega, and precipitation fields for each model time step over a 36-h time interval. The analysis was first made for idealized cases to dem-

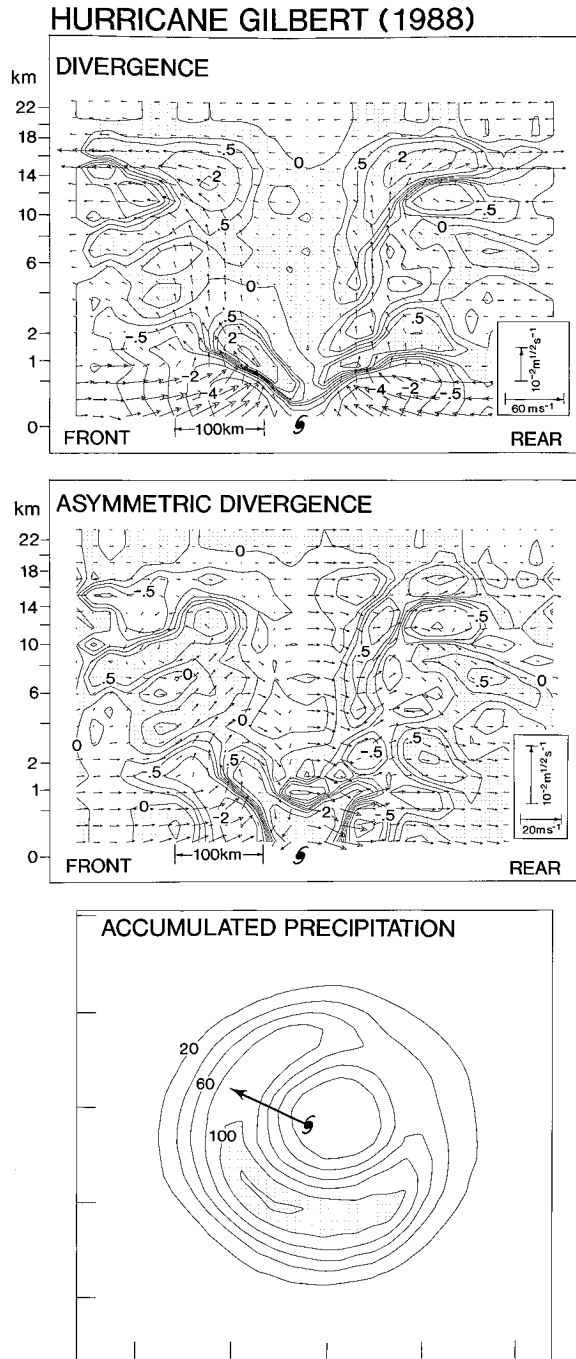


FIG. 17. Vertical cross sections through the storm center and in the direction of the storm motion of the 36-h averaged radial-vertical flow field and the total divergence (top, 10^{-4} s^{-1}), the asymmetric relative wind-asymmetric vertical flow field ($\bar{\mathbf{v}}_{\text{asym}} - \mathbf{C}$, $\bar{\mathbf{w}}_{\text{asym}}$) and asymmetric divergence (middle, 10^{-4} s^{-1}), and the distribution of the 36-h accumulated precipitation (bottom, cm) for the case of Hurricane Gilbert (1988). Regions of positive values of divergence or asymmetric divergence and accumulated precipitation greater than 100 cm are indicated with light shading. The storm direction is indicated in the bottom panel by the thick arrow. See Fig. 1 for more details.

onstrate the importance of the relative flow in the evolution of the quasi-steady, asymmetric structure in these idealized storms. The analysis procedure used in these experiments was then applied to one real case of Hurricane Gilbert (1988) to demonstrate that the relationship between the relative flow and the quasi-steady asymmetric structure analyzed in the idealized studies could be identified in this real data case.

Similar to the observational studies, analysis of the various experiments confirmed that the vertical profile of the asymmetric wind is one of the key factors in determining the structure of quasi-steady asymmetries in the interior region of tropical cyclones. The results of vorticity budget analysis indicate that steady forcing on the vorticity field of the storm was caused by the vorticity advection due to the difference between the asymmetric wind and the storm motion. This forcing was balanced with vorticity stretching and compression due to the asymmetric wind. Asymmetries in convergence and divergence, vertical motion, and accumulated precipitation were closely related to the field of vorticity stretching. This confirmed the importance of the mechanism of vorticity stretching and compression that was suggested by Willoughby et al. (1984).

The time-averaged vortex structure was nearly axisymmetric in an experiment with constant f and no basic flow. When the variation of f was included, beta-gyre flow was generated that was strongest in the inner region just above the boundary layer and steadily decreased with height. This asymmetric flow in the lower part of the free atmosphere exceeded the storm's translational speed from the boundary layer to around 6 km, which caused relative flow into the eyewall from the south-southeast and out of the eyewall on the north-northwest side. Evaluation of several terms in the vorticity equation indicated that a large vorticity tendency with magnitude of $1-2 \times 10^{-7} \text{ s}^{-2}$ was produced through advection of the symmetric vorticity by the relative flow in the lower free atmosphere of the eyewall region where the vorticity gradient was large. To counterbalance this steady forcing, a persistent area of vorticity compression and asymmetric divergence ($\sim 1 \times 10^{-4} \text{ s}^{-1}$) existed ahead of the propagating storm with an area of vorticity stretching and convergence in the lower free atmosphere of the rear eyewall. These asymmetries in the divergence field were consistent with quasi-steady asymmetries in the distributions of upward motion at middle levels and accumulated precipitation in the eyewall region. Specifically, the accumulated rainfall as well as the middle-level upward motion had a maximum value to the rear of the eyewall. This was a favored region for the intensification of the precipitation cells that tended to rotate cyclonically around the storm center and weaken in the region of divergence, in the northwest eyewall. These results suggest that, among many different factors contributing to the observed asymmetries that evolve in real tropical cyclones, the vertical profile of the asymmetric wind due to the beta gyre may be an important

one when the environmental flow is very weak. This experiment also clearly suggests an important relationship between the vertical profile of the relative flow and the quasi-steady asymmetric fields of convergence and divergence in the interior of tropical cyclones.

Since the environmental flow, especially with vertical shear, will also have a large impact on the relative flow into and out of a tropical cyclone, this effect was investigated in experiments performed with constant f and with simple easterly flows. The first experiment was run with a constant basic flow with height, the second with easterly shear above the boundary layer. In the case with an initially constant basic flow of 5 m s^{-1} , maximum boundary layer convergence developed in the front side of the storm, associated with the region of maximum relative inflow. However, interaction of the basic flow with the vortex also increased the magnitude of the basic flow just above the boundary layer, resulting in flow into and out of the storm between 1 and 3 km. This produced divergence (convergence) in the free atmosphere in the front (rear) of the storm. This divergent-convergent pattern in the lower free atmosphere had a significant impact in the upward motion at middle levels in the eyewall, masking the effect of the asymmetries in the boundary layer convergence underneath. Hence, the accumulated precipitation exhibited a small increase ($\sim 35 \text{ cm}$) to the rear of the storm, compared to the front side. It is uncertain how much the interaction of the vortex with the basic flow observed in this experiment is found in real storms as well. This remains a topic for further study. Nevertheless, this result again demonstrates the important correlation that exists between the relative wind and asymmetries in the storm interior.

In the vertical shear experiment, the relative wind was from the front to the rear of the storm from the surface to 4 km and averaged about 8 m s^{-1} in the boundary layer. Above 5 km, strong relative flow occurred from the rear to the front of the storm. The strong relative flow was associated with large vorticity stretching ahead and vorticity compression to the rear of the vortex in the lower part of the atmosphere, and the magnitude of the asymmetric boundary layer convergence and divergence was more than doubled in these regions compared to the constant easterly flow case. Similarly, in the outflow layer, where the relative wind acted in the opposite direction, the divergent outflow was significantly increased in the front side of the storm and reduced in the rear. As a result of both effects, the upward motion was significantly increased in the front of the storm and reduced in the rear, and the precipitation maximum shifted to the left front quadrant of the storm.

Observed studies have indicated the tendency for maximum convective activity to be often located ahead of translating tropical cyclones. The present results suggest that this observed asymmetric precipitation distribution is greatly influenced by the direction and magnitude of the relative winds in the free atmosphere

with height. Similarly, the observational studies previously cited also concluded that away from land influences, the shear of the environmental wind is a key factor controlling the asymmetric distribution of convection in the hurricane eyewall, rather than the location of the maximum inflow and boundary layer convergence in the front right quadrant as suggested by Shapiro (1983). It should be pointed out, however, that in the results of Shapiro, his model was a simple slab boundary layer model of constant depth with no vertical variation. Indeed, in the final idealized experiment in this study, run with constant easterly basic flow and variable f , the relative flow in the lower free atmosphere was from the southeast and increased to over 4 m s^{-1} . As a result, the precipitation maximum was located in the southeast sector of the storm, in contrast to the asymmetry in the boundary layer convergence underneath. This precipitation distribution was similar to the experiment with variable f and no basic flow.

Finally, when one real data case of Hurricane Gilbert was analyzed that exhibited easterly vertical environmental shear, relative flow of $5\text{--}6 \text{ m s}^{-1}$ was found in the boundary layer and $1\text{--}4 \text{ m s}^{-1}$ in the free atmosphere directed from the front to the rear of the storm. Associated with the relative flow into the storm, a region of asymmetric convergence in the front of the eyewall extended to nearly 200 km from the storm center. Consistent with the asymmetric divergent distribution, the upward motion became distinctly stronger on the front side of the eyewall, and the maximum accumulated precipitation was found in the left front quadrant. This confirms that although the present idealized experiments were performed with an idealized vortex and environmental flows, the results obtained should be applicable to real data cases. In conclusion, the effect of the relative wind is an important factor in determining the quasi-steady asymmetries in the distribution of accumulated precipitation and upward motion.

Future plans include investigation of the quasi-steady asymmetric structure in more real data cases. In particular, analysis will soon begin for several cases from the 1995 hurricane season, including Hurricanes Erin and Opal in the Gulf of Mexico, and Hurricane Felix in the central Atlantic. Some of the preliminary experiments with an ocean-coupled model have already suggested that the interaction with the ocean may play a role in modifying some of the asymmetric structure observed in these idealized cases. This will be investigated with a new version of the GFDL hurricane model that includes the effect of ocean coupling. The present study should serve as a guideline in determining the strategy and design for future numerical studies and observational analysis of the internal asymmetric structure of these tropical cyclones.

Acknowledgments. The author would like to thank J. Mahlman for his continuous support of the Hurricane Dynamics Project at GFDL. He would also like to ex-

caused by the vertical shear of the environmental wind

press his appreciation to Yoshio Kurihara, Robert E. Tuleya, Chun-Chieh Wu, Russ Elsberry, and Isidoro Orlandi for their comments and criticisms on earlier versions of this manuscript, and to Robert E. Tuleya for his useful discussions with the author. Special appreciation is given to Yoshio Kurihara for his many comments and suggestions made to the author throughout this study. Finally, special thanks and credit are given to J. Varanyak and C. Raphael for preparing the figures.

REFERENCES

- Bender, M. A., R. E. Tuleya, and Y. Kurihara, 1985: A numerical study of the effect of a mountain range on a landfalling tropical cyclone. *Mon. Wea. Rev.*, **113**, 567–582.
- , —, and —, 1987: A numerical study of the effect of island terrain on tropical cyclones. *Mon. Wea. Rev.*, **115**, 130–155.
- , I. Ginis, and Y. Kurihara, 1993a: Numerical simulations of tropical cyclone–ocean interaction with a high resolution coupled model. *J. Geophys. Res.*, **98**, 23 245–23 263.
- , R. J. Ross, R. E. Tuleya, and Y. Kurihara, 1993b: Improvements in tropical cyclone track and intensity forecasts using the GFDL initialization system. *Mon. Wea. Rev.* **121**, 2046–2061.
- Burpee, R. W., and M. L. Black, 1989: Temporal and spatial variations of rainfall near the centers of two tropical cyclones. *Mon. Wea. Rev.*, **117**, 2204–2218.
- Chan, J. C., and R. T. Williams, 1987: Analytical and numerical studies of the beta-effect in tropical cyclone motion. Part 1: Zero mean flow. *J. Atmos. Sci.*, **44**, 1257–1265.
- Chow, S., 1971: A study of the wind field in the planetary boundary layer of a moving tropical cyclone. M.S. thesis, Dept. of Meteorological Oceanography, New York University, 59 pp. [Available from NOAA/ NHRL Library, 1320 South Dixie Highway, Coral Gables, FL 33146.]
- Cline, I. M., 1926: *Tropical Cyclones*. MacMillan, 301 pp.
- Fiorino, M., and R. L. Elsberry, 1989: Some aspects of vortex structure related to tropical cyclone motion. *J. Atmos. Sci.*, **46**, 975–990.
- Frank, W. M., 1977: The structure and energetics of the tropical cyclone. Part 1: Storm structure. *Mon. Wea. Rev.*, **105**, 1119–1135.
- , 1984: A composite analysis of the core of a mature hurricane. *Mon. Wea. Rev.*, **112**, 2401–2420.
- Franklin, J. L., S. J. Lord, and F. D. Marks Jr., 1988: Dropwindsonde and radar observations of the eye of Hurricane Gloria (1985). *Mon. Wea. Rev.*, **116**, 1237–1244.
- , —, S. E. Feuer, and F. D. Marks Jr., 1993: The kinematic structure of Hurricane Gloria (1985) determined from nested analyses of dropwindsonde and Doppler radar data. *Mon. Wea. Rev.*, **121**, 2433–2451.
- Holland, G., 1984: Tropical cyclone motion: A comparison of theory and observation. *J. Atmos. Sci.*, **41**, 68–75.
- Houze, R. A., Jr., F. D. Marks Jr., and R. A. Black, 1992: Dual-aircraft investigation of the inner core of Hurricane Norbert. Part II: Mesoscale distribution of ice particles. *J. Atmos. Sci.*, **49**, 943–962.
- Kurihara, Y., 1973: A scheme of moist convective adjustment. *Mon. Wea. Rev.*, **101**, 547–553.
- , and M. A. Bender, 1980: Use of a movable nested mesh model for tracking a small vortex. *Mon. Wea. Rev.*, **108**, 1792–1809.
- , —, R. E. Tuleya, and R. J. Ross, 1990: Prediction experiments of Hurricane Gloria (1985) using a multiply nested movable mesh model. *Mon. Wea. Rev.*, **118**, 2185–2198.
- , —, and R. J. Ross, 1993: An initialization scheme of hurricane models by vortex specification. *Mon. Wea. Rev.*, **121**, 2030–2045.
- Marks, F. D., Jr., 1985: Evolution of the structure of precipitation in Hurricane Allen (1980). *Mon. Wea. Rev.*, **113**, 909–930.
- , R. A. Houze Jr., and J. F. Gamache, 1992: Dual-aircraft investigation of the inner core of Hurricane Norbert. Part I: Kinematic structure. *J. Atmos. Sci.*, **49**, 919–942.
- Mellor, G. L., and T. Yamada, 1974: A hierarchy of turbulence closure models for planetary boundary layers. *J. Atmos. Sci.*, **31**, 1791–1806.
- Miller, B. I., 1958: Rainfall rates in Florida hurricanes. *Mon. Wea. Rev.*, **86**, 258–264.
- Peng, M. S., and R. T. Williams, 1990: Dynamics of vortex asymmetries and their influence on vortex motion on a β -plane. *J. Atmos. Sci.*, **47**, 1987–2003.
- Shapiro, L. J., 1983: Asymmetric boundary layer flow under a translating hurricane. *J. Atmos. Sci.*, **40**, 1984–1998.
- , 1992: Hurricane vortex motion and evolution in a three-layer model. *J. Atmos. Sci.*, **49**, 140–153.
- Smith, R. K., and W. Ulrich, 1990: An analytical theory of tropical cyclone motion using a barotropic model. *J. Atmos. Sci.*, **47**, 1973–1986.
- , —, and G. Dietachmayer, 1990: A numerical study of tropical cyclone motion using a barotropic model. Part 1. The role of vortex asymmetries. *Quart. J. Roy. Meteor. Soc.*, **116**, 337–362.
- Tuleya, R. E., M. A. Bender, and Y. Kurihara, 1984: A simulation study of the landfall of tropical cyclones using a movable nested-grid model. *Mon. Wea. Rev.*, **112**, 124–136.
- Wang, B., and X. Li, 1992: The beta drift of three-dimensional vortices: A numerical study. *Mon. Wea. Rev.*, **120**, 579–593.
- Willoughby, H. E., F. D. Marks Jr., and R. J. Feinberg, 1984: Stationary and moving convective bands in hurricanes. *J. Atmos. Sci.*, **41**, 3189–3211.
- Wu, C.-C., and K. A. Emanuel, 1993: Interaction of a baroclinic vortex with background shear: Application to hurricane movement. *J. Atmos. Sci.*, **50**, 62–76.
- , and —, 1994: On hurricane outflow structure. *J. Atmos. Sci.*, **51**, 1995–2003.